NUSC Technical Report 8753
16 July 1990

(2)

Operating Characteristics for Weighted Energy Detector with Gaussian Signals

Albert H. Nuttall
Surface ASW Directorate

Naval Underwater Systems Center
Newport, Rhode Island / New London, Connecticut

Preface

This research was conducted under NUSC Project No. A75215, Subproject No. R00N000, "Determination of Concentrated Energy Distribution Functions in the Time-Frequency Plane," Principal Investigator Dr. Albert H. Nuttall (Code 304). This technical report was prepared with funds provided by the NUSC In-House Independent Research and Independent Exploratory Development Program, sponsored by the Office of the Chief of Naval Research. Also, this report was prepared under NUSC Project No. C15430, Subproject No. 900988, "AN/BQQ-5 Performance Predictions", Principal Investigator Thomas O. Sypher (Code 2111). The sponsoring activity was the Naval Sea Systems Command (SEA-PMS 409).

The technical reviewer for this report was Erik B. Siborg (Code 2111).

Reviewed and Approved: 16 July 1990

Larry Freeman
Associate Technical Director
Surface ASW Directorate

REPORT DOCUMENTATION PAGE

Form Approved
OMB No. 0704-0188

1. AGENCY USE ONLY (Leave blank)	2. REPORT DATE	3. REPORT TYPE AND DATES COVERED
	16 July 1990	Progress

4. TITLE AND SUBTITLE
OPERATING CHARACTERISTICS FOR WEIGHTED ENERGY DETECTOR WITH GAUSSIAN SIGNALS

5. FUNDING NUMBERS
PE 61152N
PR C15430

6. AUTHOR(S)
Albert H. Nuttall

7. PERFORMING ORGANIZATION NAME(S) AND ADDRESS(ES)
Naval Underwater Systems Center
New London Laboratory
New London, CT 06320

8. PERFORMING ORGANIZATION REPORT NUMBER
TR 8753

9. SPONSORING/MONITORING AGENCY NAME(S) AND ADDRESS(ES)
Naval Sea Systems Command
Washington, DC 20362

10. SPONSORING/MONITORING AGENCY REPORT NUMBER

11. SUPPLEMENTARY NOTES

12a. DISTRIBUTION/AVAILABILITY STATEMENT
Approved for public release; distribution is unlimited.

12b. DISTRIBUTION CODE

13. ABSTRACT *(Maximum 200 words)*

The performance of several weighted energy detectors of Gaussian signals in noise are investigated, both by exact procedures and by five different approximation procedures. In particular, receiver operating characteristics, for false alarm probabilities ranging from 1E-10 to .1 and detection probabilities ranging from .01 to .999, are quantitatively compared. The standard Gaussian approximation is found to be severely deficient and generally optimistic for small false alarm probabilities, while two different fourth-order approximations have excellent capability over the entire range of probabilities considered.

A method of avoiding the calculation of the eigenvalues of a covariance matrix, and yet accurately predicting performance of a fading medium, is presented. It requires only sums of products of the covariance elements directly, the precise number depending on the order of the approximation.

14. SUBJECT TERMS		15. NUMBER OF PAGES
Operating Characteristics	Gaussian Signals	
Weighting	Characteristic Function	16. PRICE CODE
Energy Detection	False Alarm Probability	

17. SECURITY CLASSIFICATION OF REPORT	18. SECURITY CLASSIFICATION OF THIS PAGE	19. SECURITY CLASSIFICATION OF ABSTRACT	20. LIMITATION OF ABSTRACT
UNCLASSIFIED	UNCLASSIFIED	UNCLASSIFIED	UL

14. Subject Terms (Cont'd.)

Partial Fraction Expansion
Exceedance Distribution
Chi-Squared Approximation
Gaussian Approximation
Effective Number
Cumulants
Detection Probability
Non-Central Chi-Squared

TABLE OF CONTENTS

LIST OF ILLUSTRATIONS

LIST OF SYMBOLS

M	number of envelope-squared samples, (1)
e_m	output envelope of narrowband filter, (1)
z_m	squared-envelope output of narrowband filter, (1)
w_m	weight applied to squared-envelope z_m, (1)
x	decision variable of weighted summer, (1)
r	exponential weighting decay factor, (2), (27)
p_z	probability density function of random variable z, (3)
u	argument of probability density function, (3)
R	signal-to-noise power ratio per sample, (4)
a	signal-to-noise ratio parameter, (3), (4)
f_z	characteristic function of random variable z, (5)
ξ	argument of characteristic function, (5)
E	ensemble average, (5)
$\chi_z(k)$	k-th cumulant of random variable z, (6)
f_x	characteristic function of random variable x, (7)
$\chi_x(k)$	k-th cumulant of random variable x, (8)
W_k	sum of k-th powers of weights w_m, (8), (36)
μ_x	mean of random variable x, (9)
λ_m	m-th eigenvalue of covariance matrix, (10), (45)
σ^2	variance, (9), (10)
D	order of diversity, (10)
Q_x	exceedance distribution function of x, (14)
e_n	partial exponential, (15)
E_n	auxiliary function, (16)
T	threshold for comparison with decision variable x, (17)

P_F	false alarm probability, (17)
P_D	detection probability, (18)
B_m	coefficient in partial fraction expansion, (21), (22)
A_m	$1/(w_m a)$, (23)
f_e	approximate chi-squared characteristic function, (28)
M_e	effective number of envelope-squared samples, (28)
w_e	effective weight, (28)
Γ	gamma function, (29)
f_c	generalized chi-squared approximation, (33)
M_c	effective number of samples, (33)
t	auxiliary parameter = r^M, (40)
P	normalized covariance matrix of fading signal, (45),(46)
tr	trace of matrix, (46)
f_d	generalized chi-squared approximation, (48)
$B_m(R)$	coefficient in partial fraction expansion, (51), (52)
ρ	covariance coefficient for $P = [\rho_{mn}]$: $\rho_{mn} = \rho^{\lvert m-n \rvert}$.
f_f	fourth-order characteristic function fit, (55)
f_g	generalized non-central chi-squared fit, (58)
R_m	signal-to-noise ratio on m-th sample, (62), (63)
N	number of signal samples, (63)
$\tilde{f}$	noise-only characteristic function, (64)
B	block size, (74)
J	number of blocks occupied by signal, (75)
ROC	receiver operating characteristic
Φ	cumulative Gaussian distribution, (A-5)
$\underset{\sim}{\Phi}$	inverse Φ function, (A-9)
Λ	diagonal matrix of eigenvalues, (C-1)

OPERATING CHARACTERISTICS FOR WEIGHTED ENERGY DETECTOR WITH GAUSSIAN SIGNALS

INTRODUCTION

The operating characteristics of an equi-weighted energy detector for Gaussian signals in noise, in terms of false alarm and detection probabilities, can be characterized mathematically by a partial exponential expansion, and have previously been numerically evaluated for arbitrary numbers of samples and signal-to-noise ratios [1; (7) - (8) and figures 2 - 6]. However, when the weights employed in the energy detector are unequal, or if the signal and noise powers on each sample are unequal, these results do not apply and can be misleading, especially when the number of samples summed is not large. What is needed, in this case of arbitrary numbers of samples and unequal weights or powers, is an exact approach in terms of the characteristic function of the decision variable; this latter function is frequently available in closed form and can be employed in the fast efficient procedure presented in [2] and utilized in [3,4,5] for direct accurate evaluation of the exceedance distribution function.

At the same time, it would be very useful to have accurate approximations for the receiver operating characteristics, which apply over the full range of applicable false alarm and detection probabilities, yet are easily computed in terms of readily available functions, or circumvent some of the more difficult

numerical procedures required in the exact approach. Here, we will consider four such approximations, namely Gaussian, chi-square, constant plus chi-square, and generalized noncentral chi-square, and demonstrate the range of applicability of each.

Thus, our goals here are two-fold

(1) determination of exact operating characteristics of arbitrary weighted energy detectors along with working programs, thereby allowing for investigation of other similar cases of interest to the user; and

(2) construction of accurate simple approximations to the operating characteristics, which can be extended to related difficult problems and/or circumvent complicated numerical procedures.

As a by-product, the inadequacy of some extant approximations will be delineated quantitatively; in particular, the generally optimistic results predicted by the Gaussian approximation will be shown to prevail even when the number of independent samples involved in the energy detector is very large.

CHARACTERISTIC FUNCTION

We presume that we have M channels (or samples) containing either noise-alone or signal-plus-noise, and that the random variables in each channel are statistically independent of each other. Specifically, for our interest, the output envelopes, $\{e_m\}$ for $1 \leq m \leq M$, of M disjoint narrowband filters are subjected to weighted square-law summation for purposes of threshold comparison and a statement about signal presence or absence on that particular observation of M outputs. The decision variable in this case is

$$x = \sum_{m=1}^{M} w_m \, e_m^2 = \sum_{m=1}^{M} w_m \, z_m \ , \qquad (1)$$

where weights $\{w_m\}$ are all positive but otherwise arbitrary, and the M squared-envelope outputs $\{z_m\}$ are statistically independent and identically distributed. An example is afforded by a finite-time exponential summer where $w_m = A \, r^{m-1}$, $r \leq 1$, $1 \leq m \leq M$.

Without loss of generality, the sum of the weights is set equal to unity,

$$\sum_{m=1}^{M} w_m = 1 \ ; \quad \text{that is,} \quad A = \frac{1-r}{1-r^M} \ . \qquad (2)$$

Then, the mean of random variable x in (1) is equal to the mean of each random variable z_m, because all the $\{z_m\}$ are identically distributed. (If there are scaling differences in the variables $\{z_m\}$, these factors can be absorbed in modified scalings $\{w_m\}$,

without loss of generality.) Under these assumptions, it should be observed that the performance of the weighted energy detector in (1) is independent of the ordering of the weights; thus, the weights can be arranged in any order without affecting the detection capability. Also, the absolute level of the $\{w_m\}$ cannot affect the operating characteristics of detector (1).

STATISTICS OF z_m

For Gaussian signals and noises present at the inputs to the M narrowband filters in (1), the probability density function of each filter output envelope-squared random variable z_m is

$$p_z(u) = \frac{1}{a} \exp\left(\frac{-u}{a}\right) \quad \text{for } u > 0 \ , \tag{3}$$

where parameter

$$a = \left\{ \begin{array}{ll} 1 & \text{for noise-alone} \\ 1 + R & \text{for signal-plus-noise} \end{array} \right\} . \tag{4}$$

Here, we have normalized according to the noise power; that is, the mean of random variable z_m is set equal to 1 for noise-alone. This presumption is equivalent to having knowledge of the average noise level in the absence of signal and can be accomplished in practice by monitoring the filter outputs over a sufficiently long past interval of time. Also, R is the signal-to-noise power ratio per sample at the output of each filter.

The characteristic function of each random variable z_m in (1) is given by expectation (ensemble average)

$$f_z(\xi) = E\{\exp(i\xi z)\} = \int du\, \exp(i\xi u)\, p_z(u) = \frac{1}{1 - i\xi a} , \qquad (5)$$

where we used (3). The cumulants $\{\chi_z(k)\}$ of z_m are immediately available from (5) as

$$\frac{1}{(k-1)!}\, \chi_z(k) = a^k \quad \text{for } k \geq 1 . \qquad (6)$$

Actually, these are scaled cumulants, by the factor $1/(k-1)!$; they are more convenient and will be employed henceforth.

CHARACTERISTIC FUNCTION OF OUTPUT x

The characteristic function of summation random variable x in (1) is given by expectation

$$f_x(\xi) = E\{\exp(i\xi x)\} = \prod_{m=1}^{M} f_z(w_m \xi) = \left[\prod_{m=1}^{M} \left(1 - i\xi w_m a\right)\right]^{-1} , \qquad (7)$$

where we used the independence of the $\{z_m\}$ and relation (5). The (scaled) cumulants of x are available from (7) according to

$$\frac{1}{(k-1)!}\, \chi_x(k) = a^k \sum_{m=1}^{M} w_m^k \equiv a^k\, W_k \quad \text{for } k \geq 1 . \qquad (8)$$

In particular, the mean and variance of x are, upon use of (2),

$$\mu_x = \chi_x(1) = a\, W_1 = a , \quad \sigma^2 = \chi_x(2) = a^2\, W_2 . \qquad (9)$$

The desired closed form for the characteristic function of x is given by (7), where the signal-to-noise ratio parameter a is given by (4). Result (7) applies for arbitrary M, weights $\{w_m\}$, and per-sample signal-to-noise ratio R.

SOME RELATED RESULTS

Characteristic functions of the form of (7) occur in numerous problems. For example, the stability of a spectral estimation technique employing overlapped FFT processing of windowed data encountered this form [6; (35) and (15)], where weights $\{w_m\}$ were proportional to the eigenvalues $\{\lambda_m\}$ of a normalized covariance function. Another example is furnished by diversity combination in a channel subject to partially-correlated signal fading; see [7; (D-14)], [8; (24)], and [9]. In particular, the exact characteristic function in [7] and [8] took the form

$$\left[\prod_{m=1}^{M}\left\{1 - i\xi\left(\sigma^2 + 2\lambda_m\right)\right\}\right]^{-D}, \qquad (10)$$

where $\{\lambda_m\}$ are the eigenvalues of a covariance matrix. Parameter D was the order of diversity in [7], but was equal to 1 in [8].

GAUSSIAN APPROXIMATION TO EXCEEDANCE DISTRIBUTION

For the general characteristic function given by (7) and (4), a Gaussian approximation to the probability density and exceedance distribution functions is given in appendix A. It is derived for arbitrary M, weights $\{w_m\}$, and signal-to-noise ratio R. However, its applicability to numerical evaluation of receiver operating characteristics, in the form of detection versus false alarm probabilities, will be shown to be rather limited in the next section.

EXCEEDANCE DISTRIBUTION FOR ALL WEIGHTS EQUAL

In this section, the weights $\{w_m\}$ in (1) and (2) are equal:

$$w_m = \frac{1}{M} \quad \text{for } 1 \le m \le M \ . \tag{11}$$

The characteristic function in (7) then becomes

$$f_x(\xi) = (1 - i\xi a/M)^{-M} \ . \tag{12}$$

This corresponds to a multiple of a chi-squared random variate with 2M degrees of freedom. The corresponding probability density function is

$$p_x(u) = \frac{u^{M-1} \exp(-uM/a)}{(M-1)!\ (a/M)^M} \quad \text{for } u > 0 \ , \tag{13}$$

while the exceedance distribution function is, for $u > 0$,

$$Q_x(u) = \int_u^\infty dt\ p_x(t) = \exp(-uM/a)\ e_{M-1}(uM/a) = E_{M-1}(uM/a) \ . \tag{14}$$

Here, $e_n(x)$ is the partial exponential function [10; (6.5.11)],

$$e_n(x) = \sum_{k=0}^{n} \frac{x^k}{k!} \ , \tag{15}$$

and we have defined auxiliary function

$$E_n(x) = \exp(-x)\ e_n(x) \quad \text{for } x \ge 0 \ . \tag{16}$$

If threshold value T is used for comparison with output x of the energy detector (1), then the false alarm probability P_F is

$$P_F = Q_x(T;\ a=1) = E_{M-1}(TM) \ . \qquad (17)$$

Similarly, the detection probability P_D is, from (14) and (4),

$$P_D = Q_x(T;\ a=1+R) = E_{M-1}\left(\frac{TM}{1+R}\right) \ . \qquad (18)$$

When T is eliminated between (17) and (18), the operating characteristics (P_D versus P_F) can be plotted, with signal-to-noise ratio R as a parameter. Separate plots are required for different values of M, the number of envelope-squared samples.

GRAPHICAL RESULTS

The receiver operating characteristics (ROC) for

$$M = 1,\ 2,\ 4,\ 8,\ 16,\ 32,\ 64,\ 128,\ 256,\ 512,\ 1024 \qquad (19)$$

are plotted in figures 1 through 11, on normal probability paper, for false alarm probabilities ranging from 1E-10 to .1 and for detection probabilities ranging from .01 to .999. Signal-to-noise ratios (in decibels) have been chosen, typically, to cover P_F,P_D possibilities from low-quality pair .01,.5 to high-quality pairs in the neighborhood of 1E-10,.99.

Superposed in figure 3 (in dashed lines) is the Gaussian approximation, for M = 4, to the exact exceedance distribution function Q_x in (14); see appendix A. Three selected values of signal-to-noise ratio R are indicated, namely R = 4, 8, and 12 dB. They are identified by a black dot where they cross the exact operating characteristic for the same signal-to-noise

ratio. It is seen that the Gaussian approximation is virtually useless at this low value of M, the number of samples.

This superposition, of three representative curves afforded by the Gaussian approximation, is continued up through M = 1024 in figure 11. Again, agreement with the exact results is generally quite poor. Even at M = 1024, the required signal-to-noise ratio from the Gaussian approximation for P_F = 1E-10, P_D = .3, for example, is in error by .3 dB.

Furthermore, it should be observed that the Gaussian approximation is always optimistic in the useful range of the operating characteristics; this bias is misleading in quantitative performance predictions applied to practical detection systems. Additionally, the case in this section, namely equal weights, is the most favorable situation for the Gaussian approximation to apply in; any other distribution of weight values makes the effective number of weights (M_e in (A-6) and sequel) less than M, thereby deviating even further from an accurate application of the central limit theorem. The message to be conveyed here is that the performance capability of energy detectors for Gaussian signals and noises should be based on something other than the Gaussian approximation.

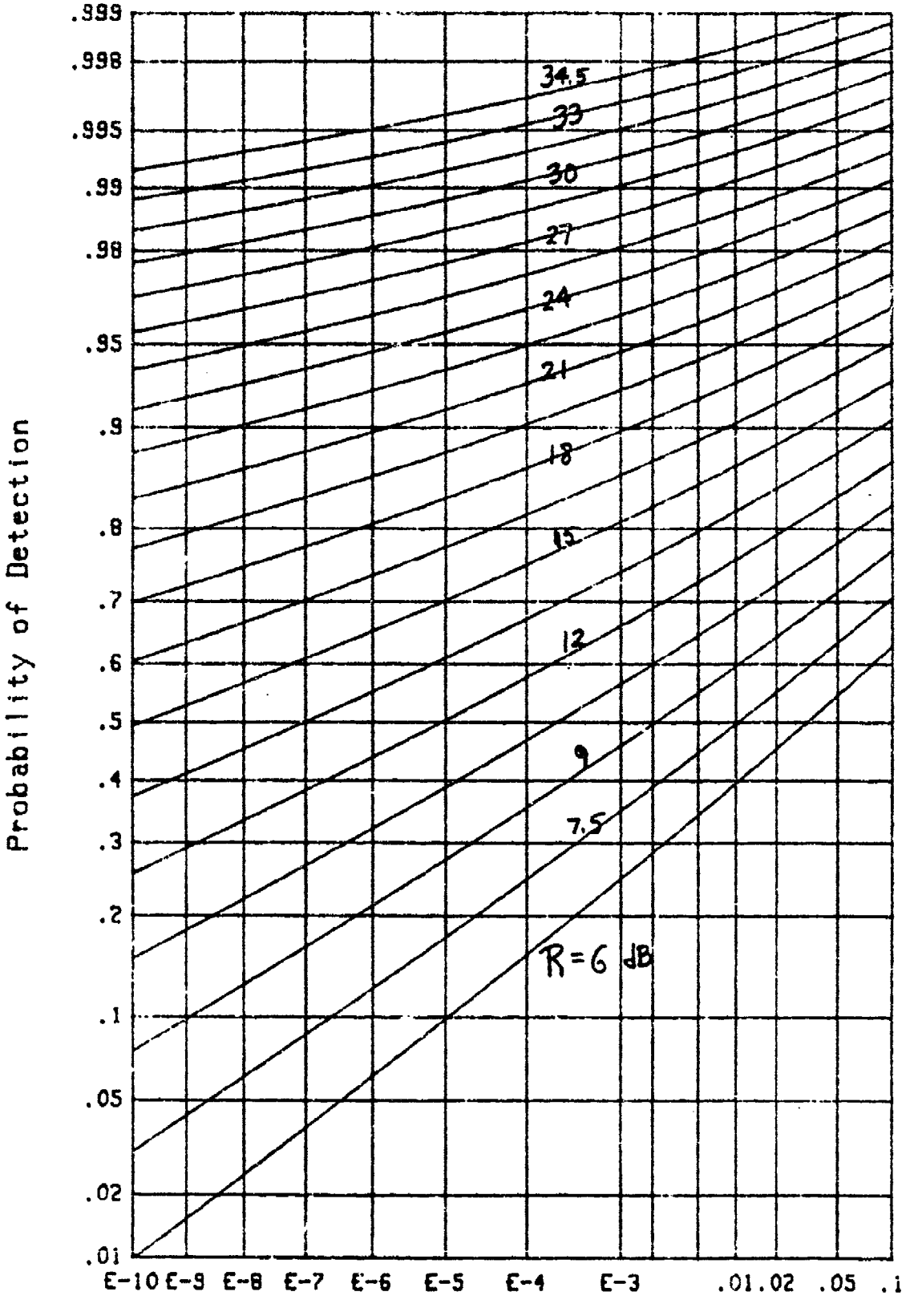

Figure 1. ROC for M=1, Equal Weights

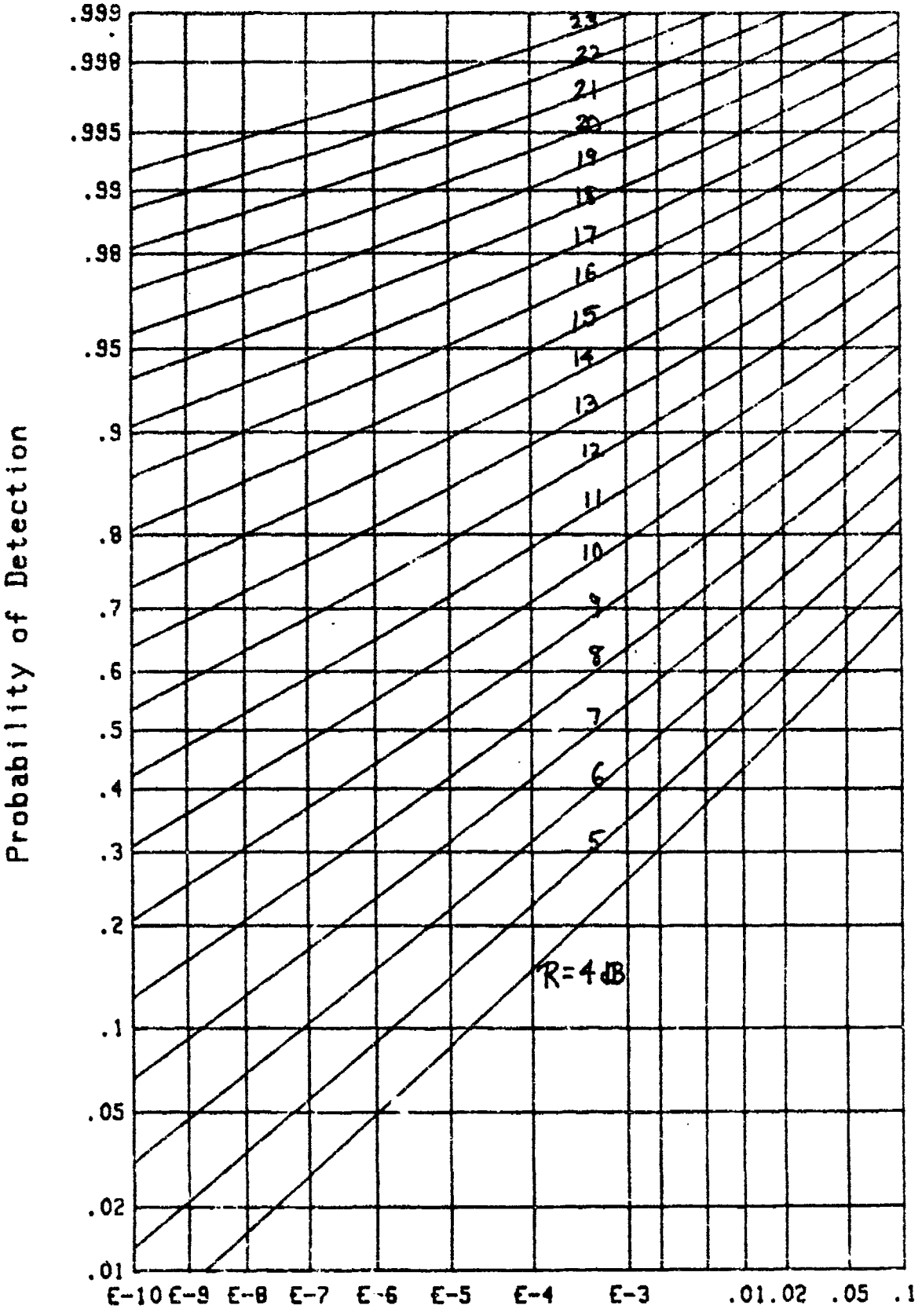

Figure 2. ROC for M=2, Equal Weights

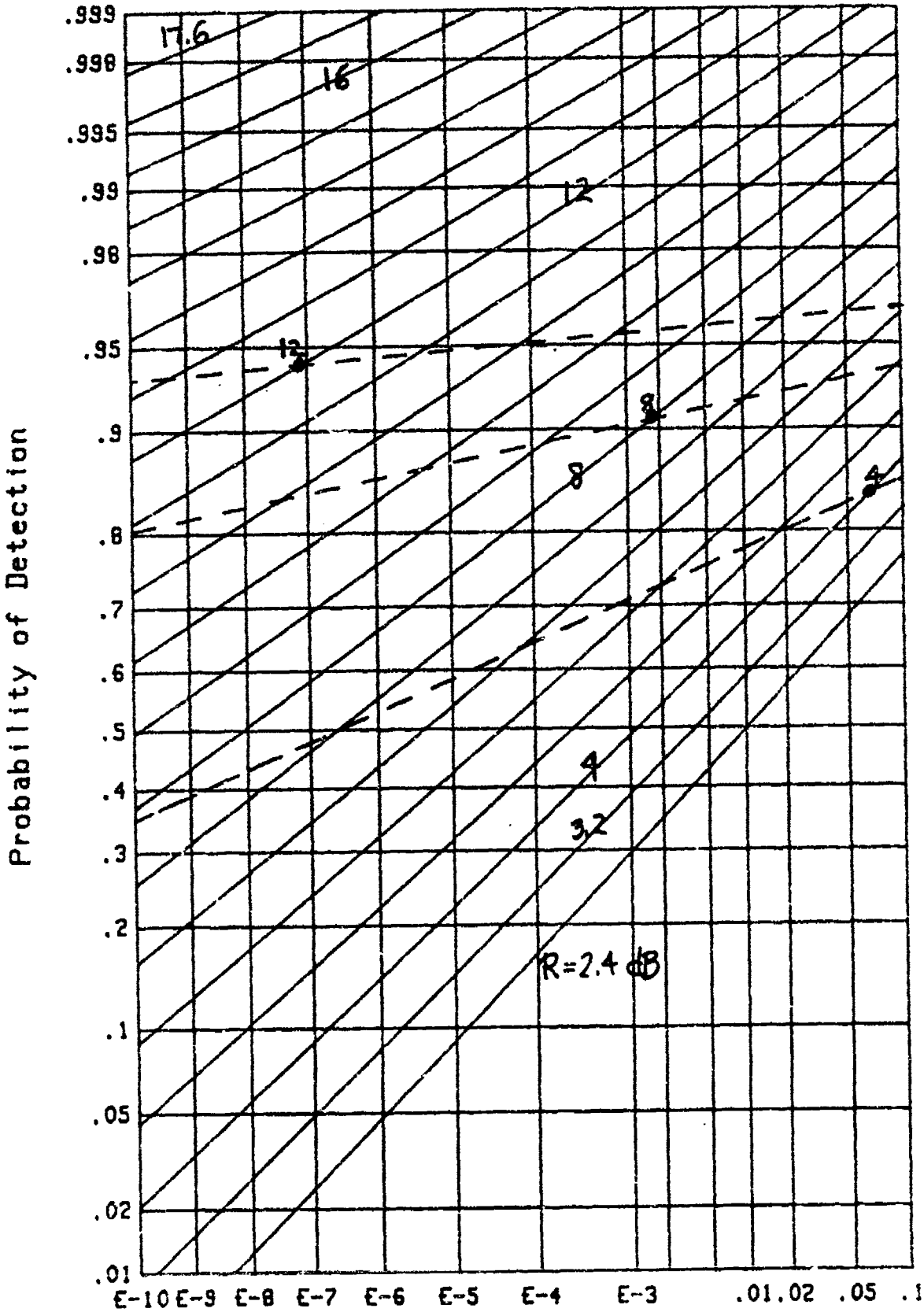

Figure 3. ROC for M=4, Equal Weights

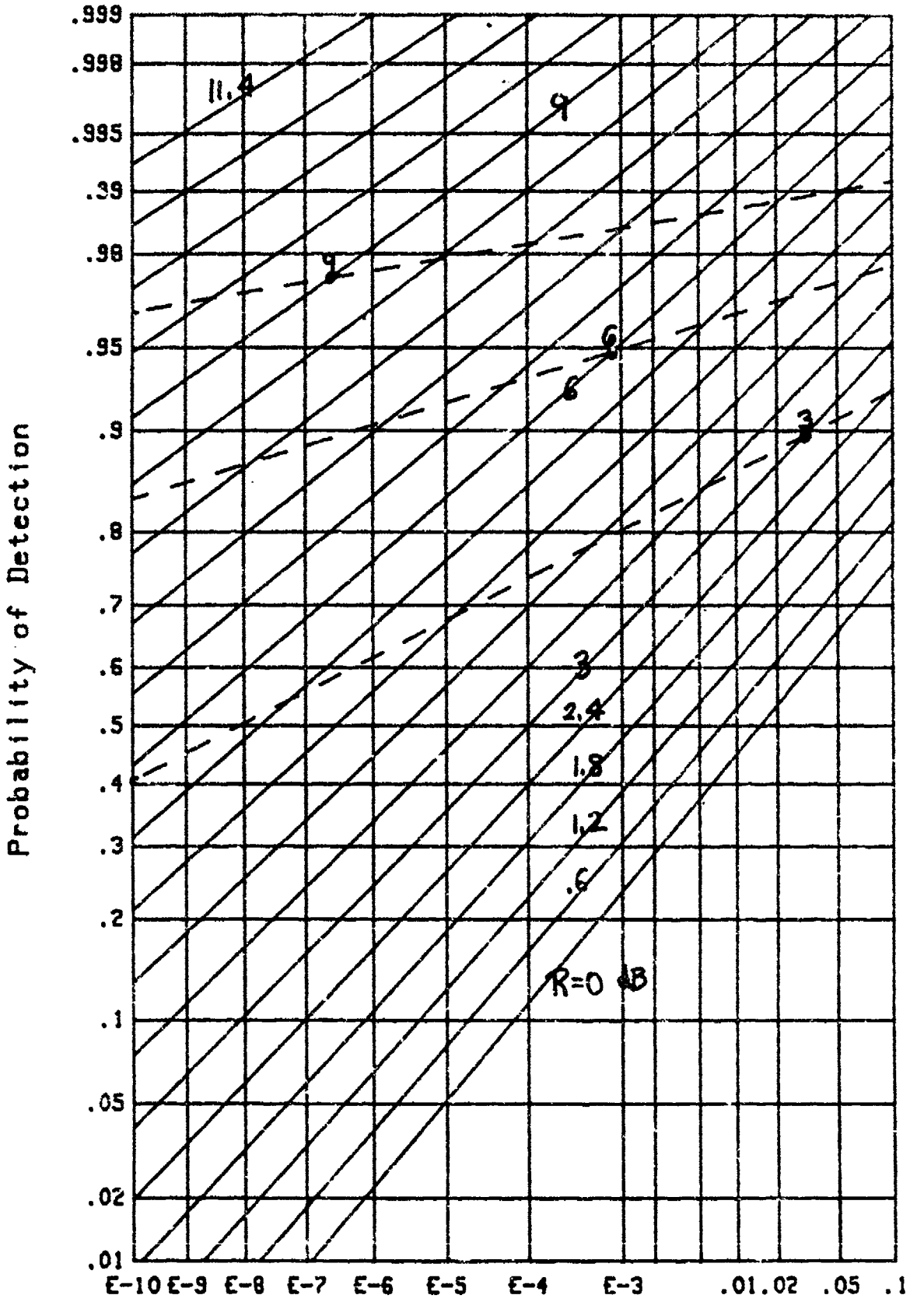

Figure 4. ROC for M=8, Equal Weights

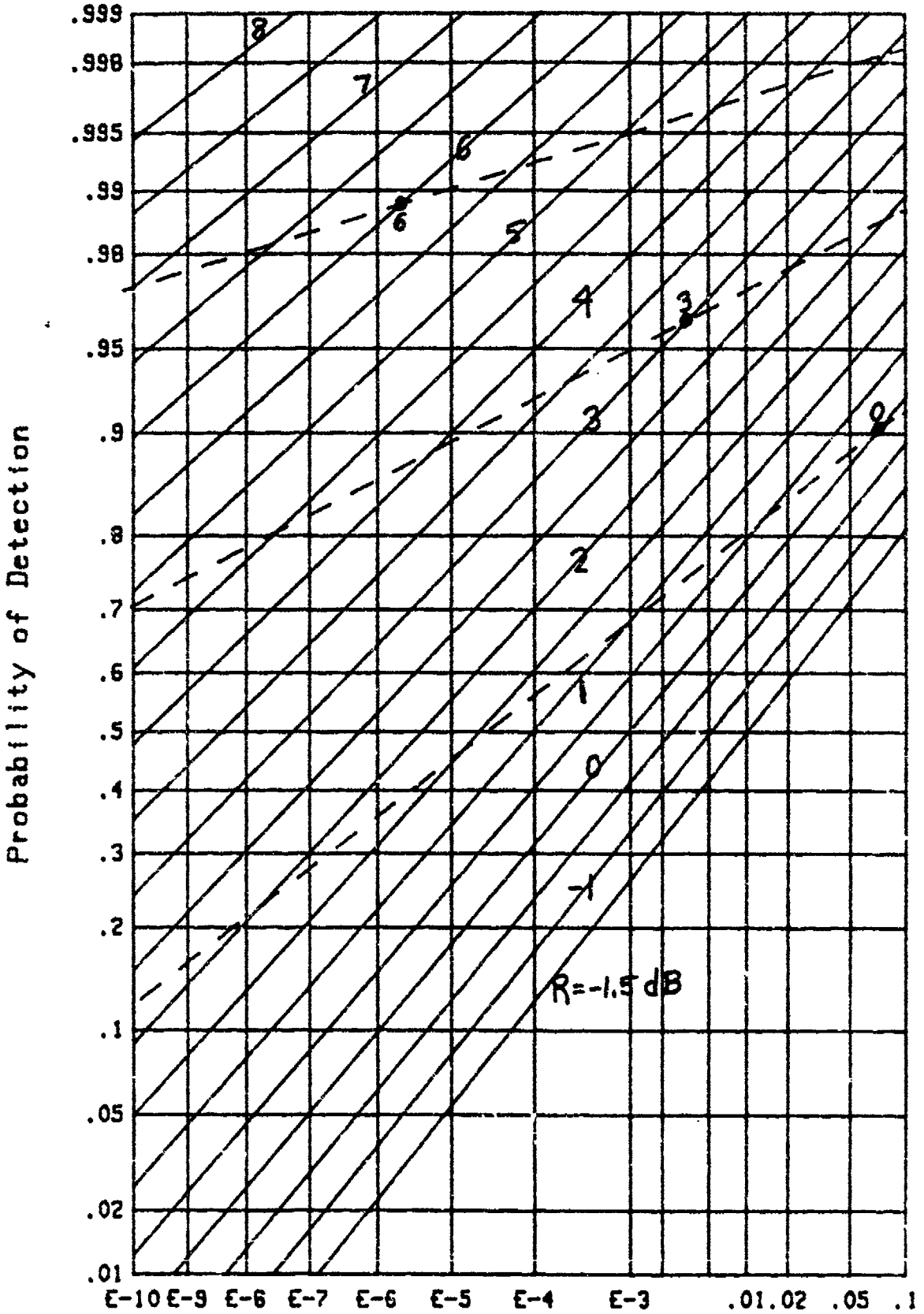

Figure 5. ROC for M=16, Equal Weights

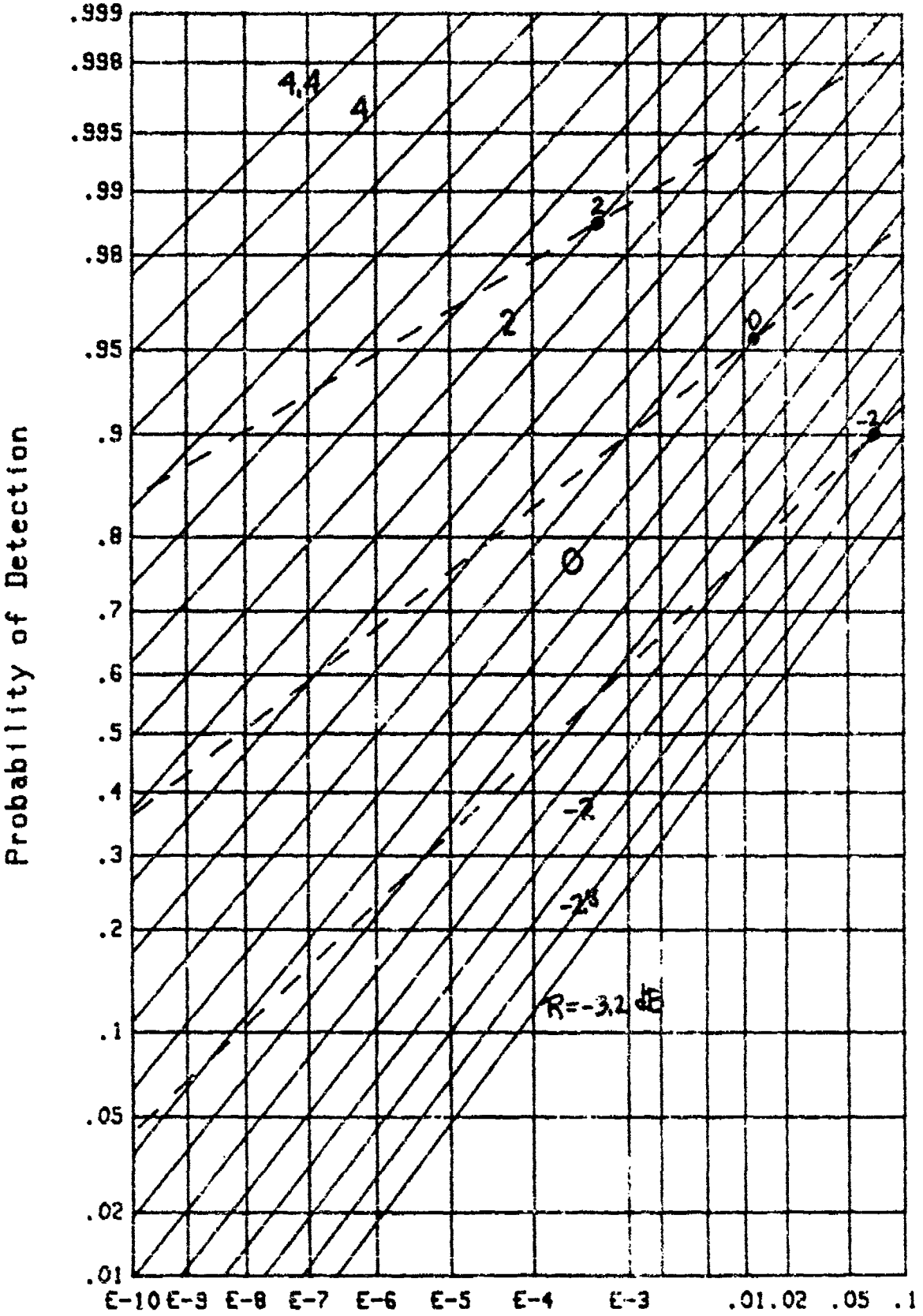

Figure 6. ROC for M=32, Equal Weights

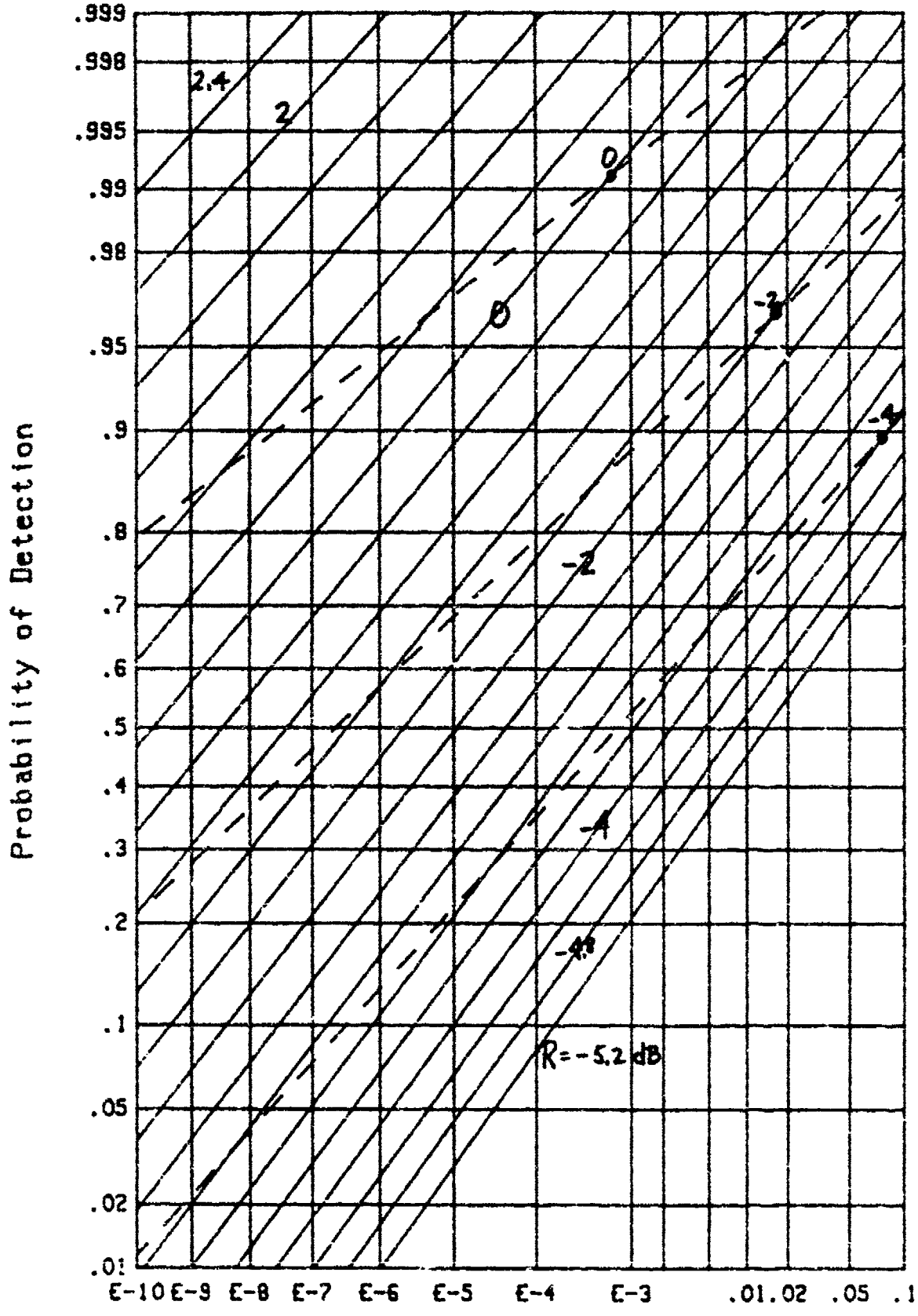

Figure 7. ROC for M=64, Equal Weights

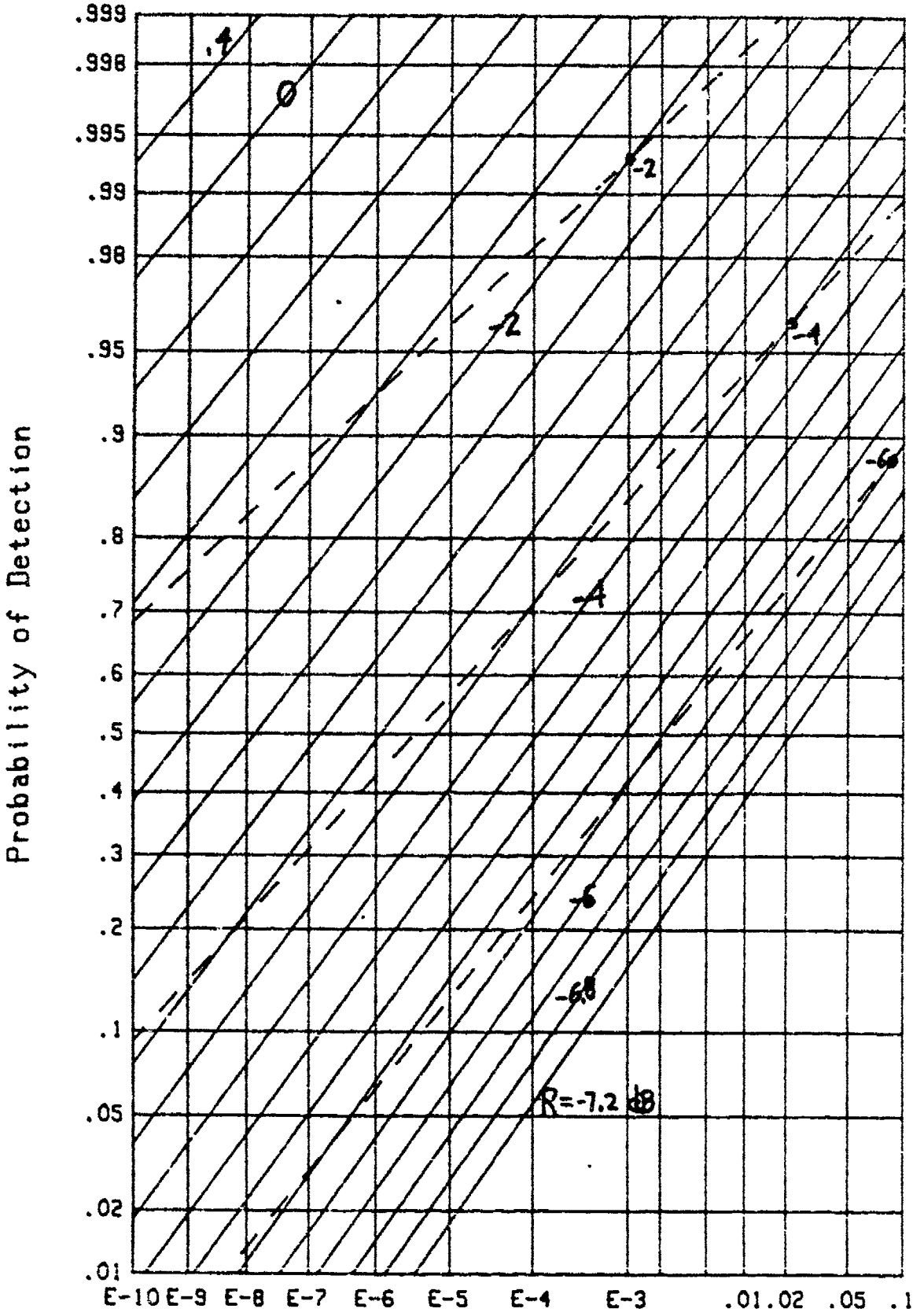

Figure 8. ROC for M=128, Equal Weights

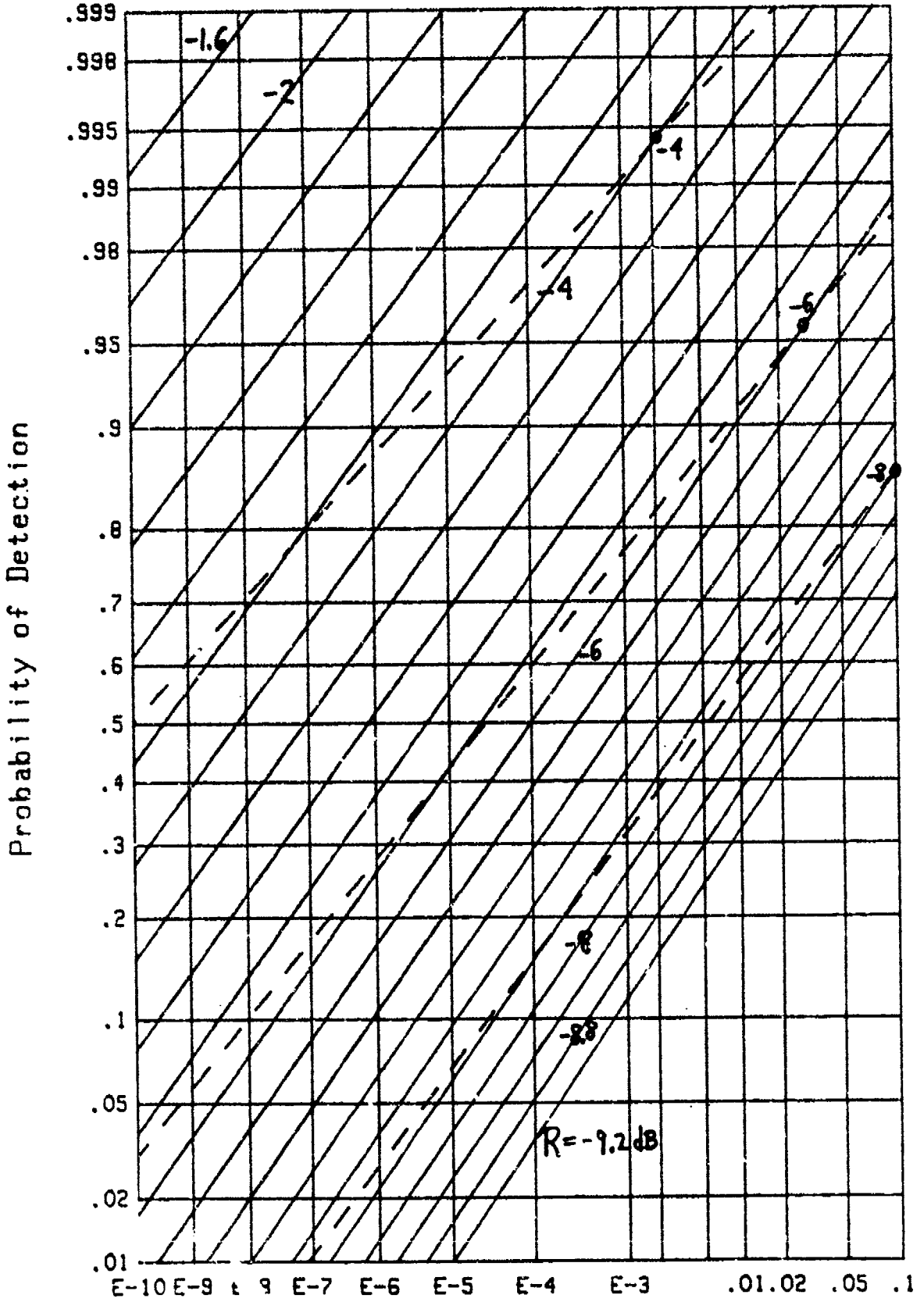

Figure 9. ROC for M=256, Equal Weights

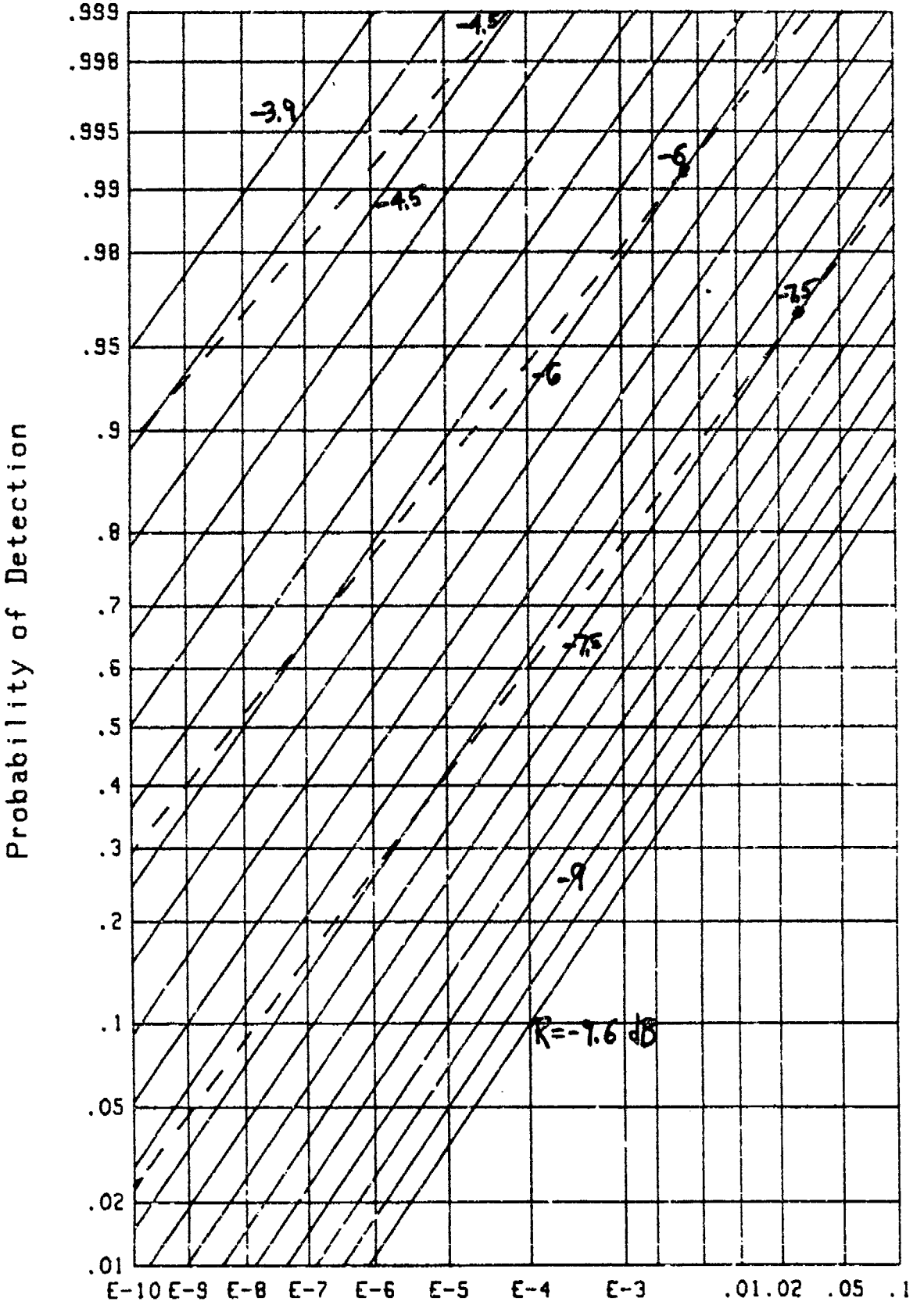

Figure 10. ROC for M=512, Equal Weights

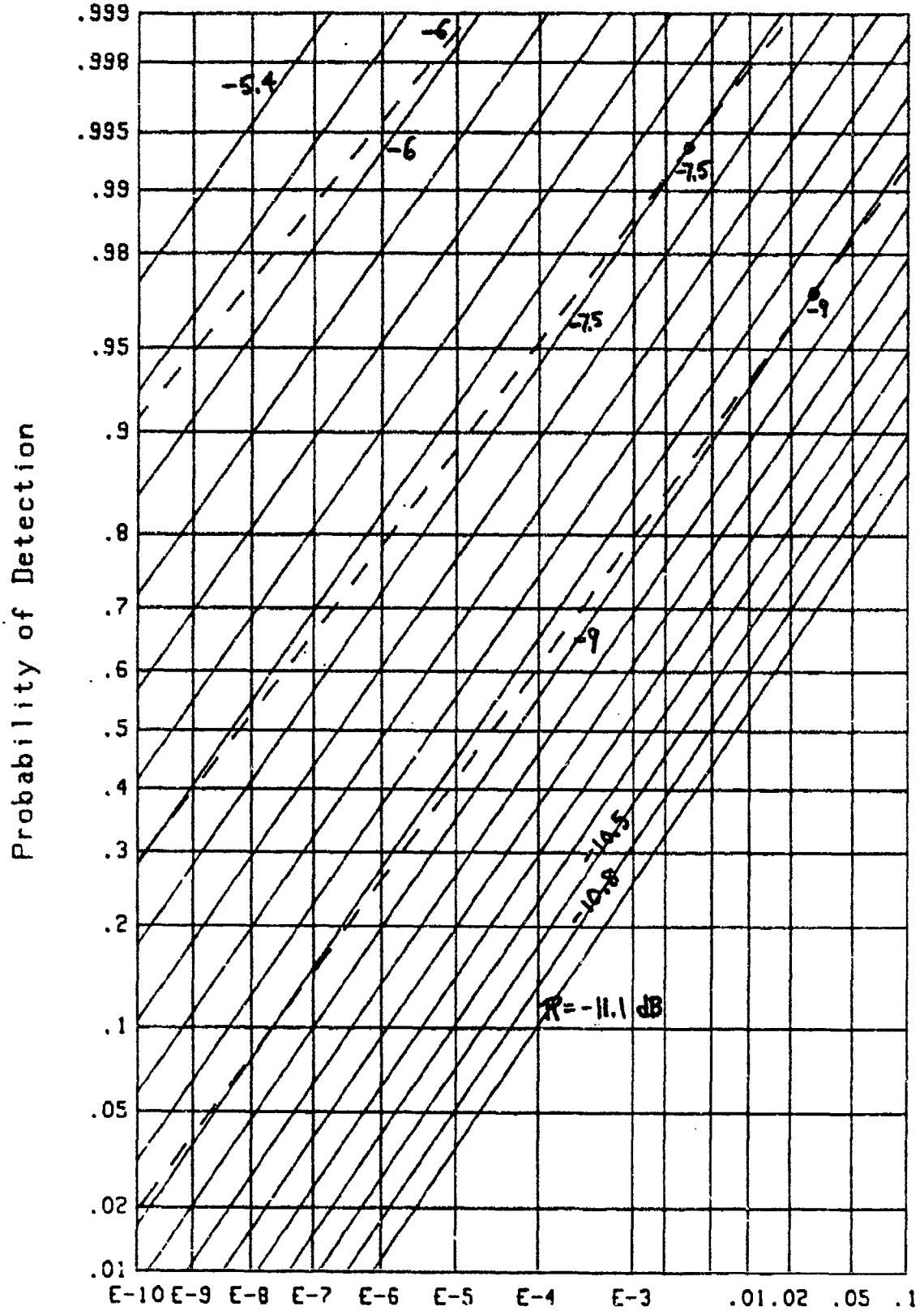

Figure 11. ROC for M=1024, Equal Weights

EXCEEDANCE DISTRIBUTION FOR ALL WEIGHTS DIFFERENT

In this section, we confine attention to the case where all the weights $\{w_m\}$ are different from each other; that is,

$$w_m \neq w_k \quad \text{if} \quad m \neq k \; ; \qquad w_m > 0 \; . \tag{20}$$

Then, we expand the characteristic function of x in (7) in a partial fraction expansion according to

$$f_x(\xi) = \left[\prod_{m=1}^{M} \left(1 - i\xi w_m a\right) \right]^{-1} = \sum_{m=1}^{M} \frac{B_m}{1 - i\xi w_m a} \; , \tag{21}$$

where coefficients

$$B_m = \frac{w_m^{M-1}}{\prod_{\substack{k=1 \\ k \neq m}}^{M} (w_m - w_k)} \qquad \text{for } 1 \leq m \leq M \; , \tag{22}$$

depend only on weights $\{w_m\}$ and not on signal-to-noise ratio R.

The probability density function of x is then immediately available from (21) as

$$p_x(u) = \sum_{m=1}^{M} A_m \, B_m \exp(-A_m u) \qquad \text{for } u > 0 \; , \tag{23}$$

where $A_m = 1/(w_m a)$. The corresponding exceedance distribution is

$$Q_x(u) = \int_u^{\infty} dt \; p_x(t) = \sum_{m=1}^{M} B_m \exp(-A_m u) \qquad \text{for } u > 0 \; . \tag{24}$$

If threshold T is used as the basis of comparison for output x of the weighted energy detector in (1), the false alarm and detection probabilities follow from (24), respectively, as

$$P_F = Q_x(T;\ a = 1)\ , \quad P_D = Q_x(T;\ a = 1 + R)\ . \tag{25}$$

As an example, if M = 1, then $w_1 = 1$, $A_1 = 1/a$, $B_1 = 1$, and (24) yields $Q_x(u) = \exp(-u/a)$ for $u > 0$. Then, (25) gives

$$P_F = \exp(-T)\ , \quad P_D = \exp\left(\frac{-T}{1+R}\right) = P_F^{\frac{1}{1+R}} = \exp\left(\frac{\ln P_F}{1+R}\right)\ . \tag{26}$$

For this special case of M = 1, threshold T can be eliminated and P_D expressed explicitly in terms of P_F and R.

GRAPHICAL RESULTS

The particular case of unequal weights that we shall concentrate on here is a set of exponential weights

$$w_m = A\ r^{m-1} \quad \text{for} \quad 1 \le m \le M\ , \quad r \le 1\ , \tag{27}$$

where scale factor A is selected for normalization of the weights, according to (2). Of course, the absolute level of the weights does not affect the operating characteristics.

In figure 12, the ROC for M = 4 and r = .99 is plotted, as determined from (25) and (24). Since r is close to 1 for this example, the weights (27) are all nearly equal, causing some of the coefficients $\{B_m\}$ in (22) to be rather large, in the range of ±.5E6. This leads to round-off error in sum (24) for the

exceedance distribution function and the possibility of useless numerical results; however, because M = 4 is a small number, the round-off error does not yet show up in figure 12.

When M is increased to 8 in figure 13 and r is kept at .99, coefficients $\{B_m\}$ in (22) reach values in the range of ±.7E12, and round-off error begins to show up as wiggly lines in the higher detection probability values near .999. We are using a computer with 64 bits per word, which yields approximately 15 decimals of accuracy for the mantissa. Although coefficients $\{B_m\}$ can be calculated very accurately from (22), they alternate in sign and can be very large. Then Q_x in (24) requires differencing of large numbers, with an attendant possibly damaging loss of accuracy, especially for small P_F.

When M is increased by one, to 9 in figure 14, and r is maintained at .99, round-off error is now significant at the upper edge of the ROC, although useful characteristics are still available for lower values of P_D. The reason for this problem is that all the weights are close to each other; in fact, the M-th weight is $r^{M-1} = .923$ times as large as the first weight. The largest coefficient values for $\{B_m\}$ are in the range of ±.16E14.

When the weights are spread out over a wider range, larger values of M can be tolerated in sum (24), without encountering significant round-off error. For example, a set of M = 16 uniformly distributed random weights, over the (0,1) interval, were utilized in figure 15 without any problems. But when M was increased to 20 in figure 16, again for uniformly distributed

weights, the upper edge of the ROC, for $P_D > .99$, was useless. Nevertheless, a significant portion of the ROC for lower P_D values is still acceptable.

The lesson to be drawn from these results is that the partial fraction expansion, leading to the exceedance distribution function in (24), has utility for spread out weights $\{w_m\}$ and moderately low values of M, the number of envelope-squared samples. However, it will not be a viable tool for large values of M, nor for general weight structures which may have some close or equal values. The more general approach presented in [2], in terms of an arbitrary characteristic function, has no such limitations, on the other hand, although the numerical calculations required are more extensive.

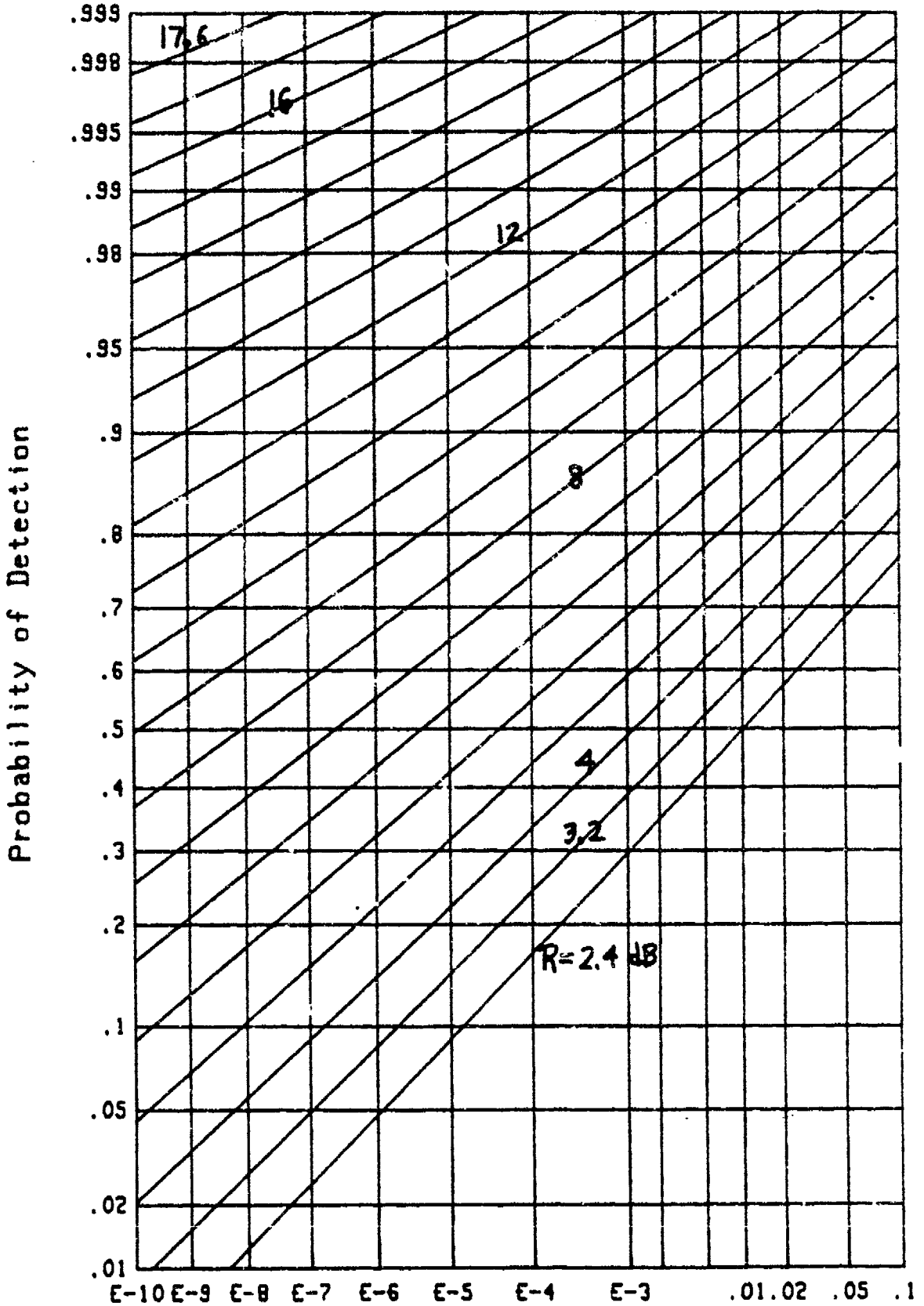

Figure 12. ROC for M=4, r=.99

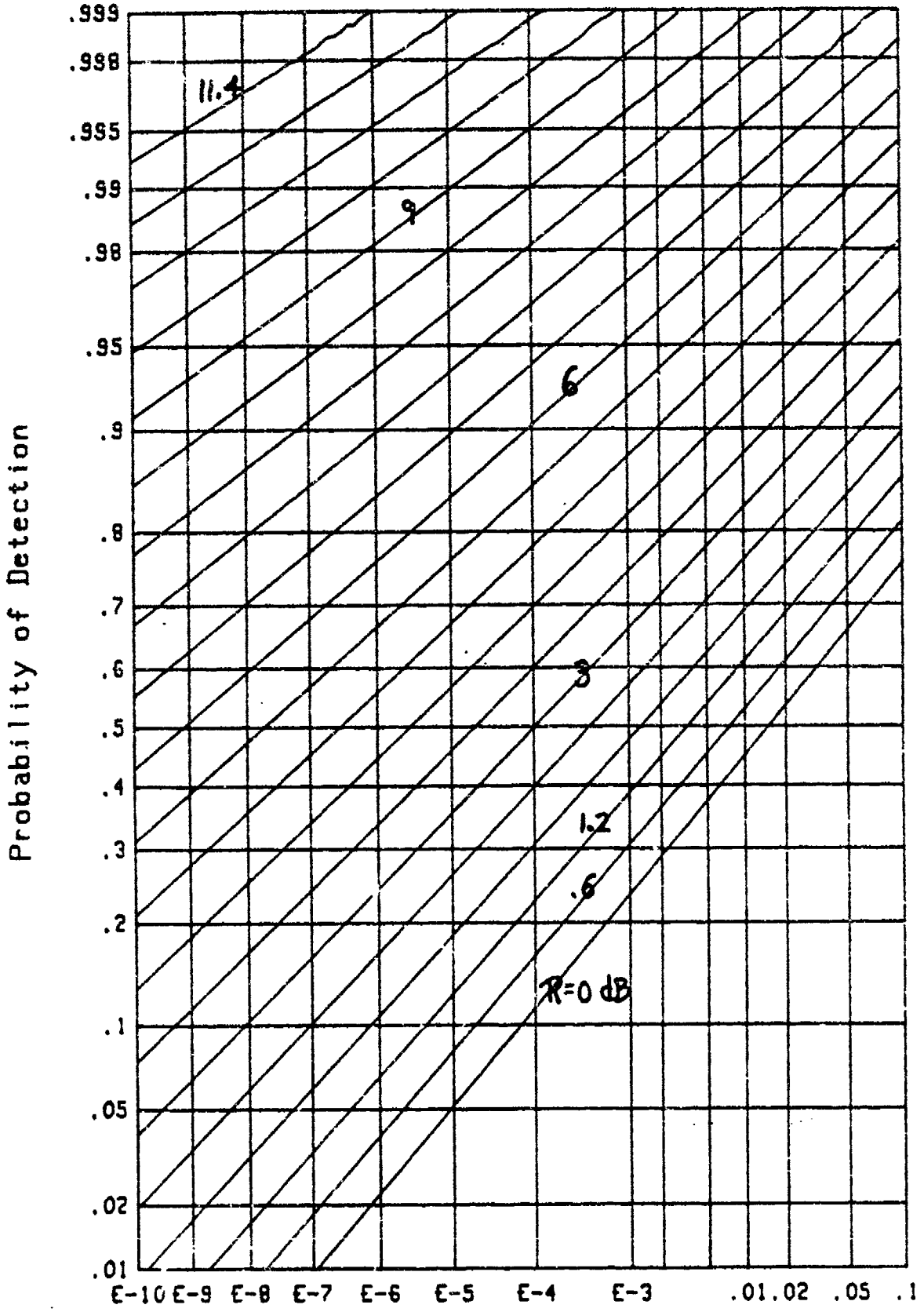

Figure 13. ROC for M=8, r=.99

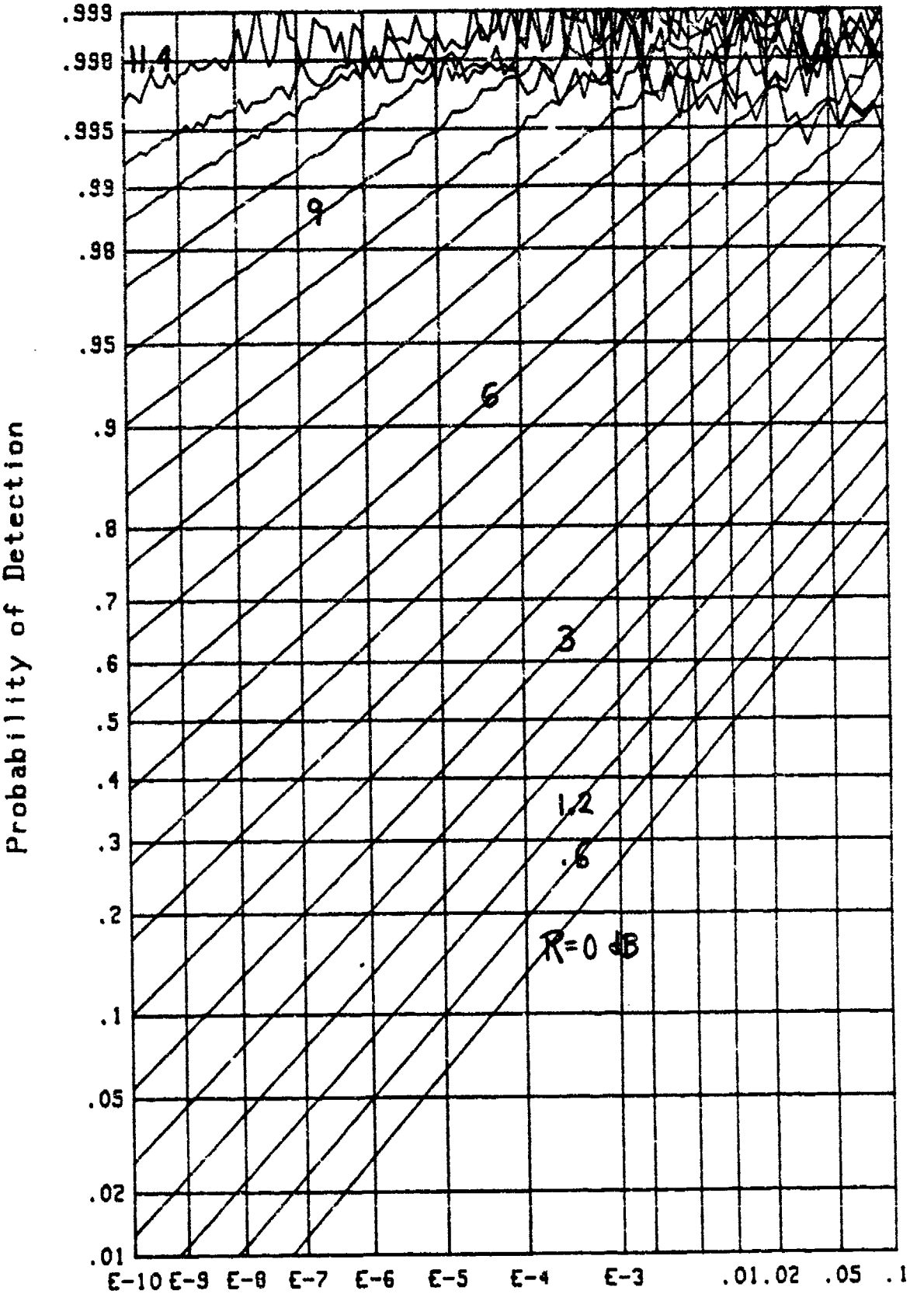

Figure 14. ROC for M=9, r=.99

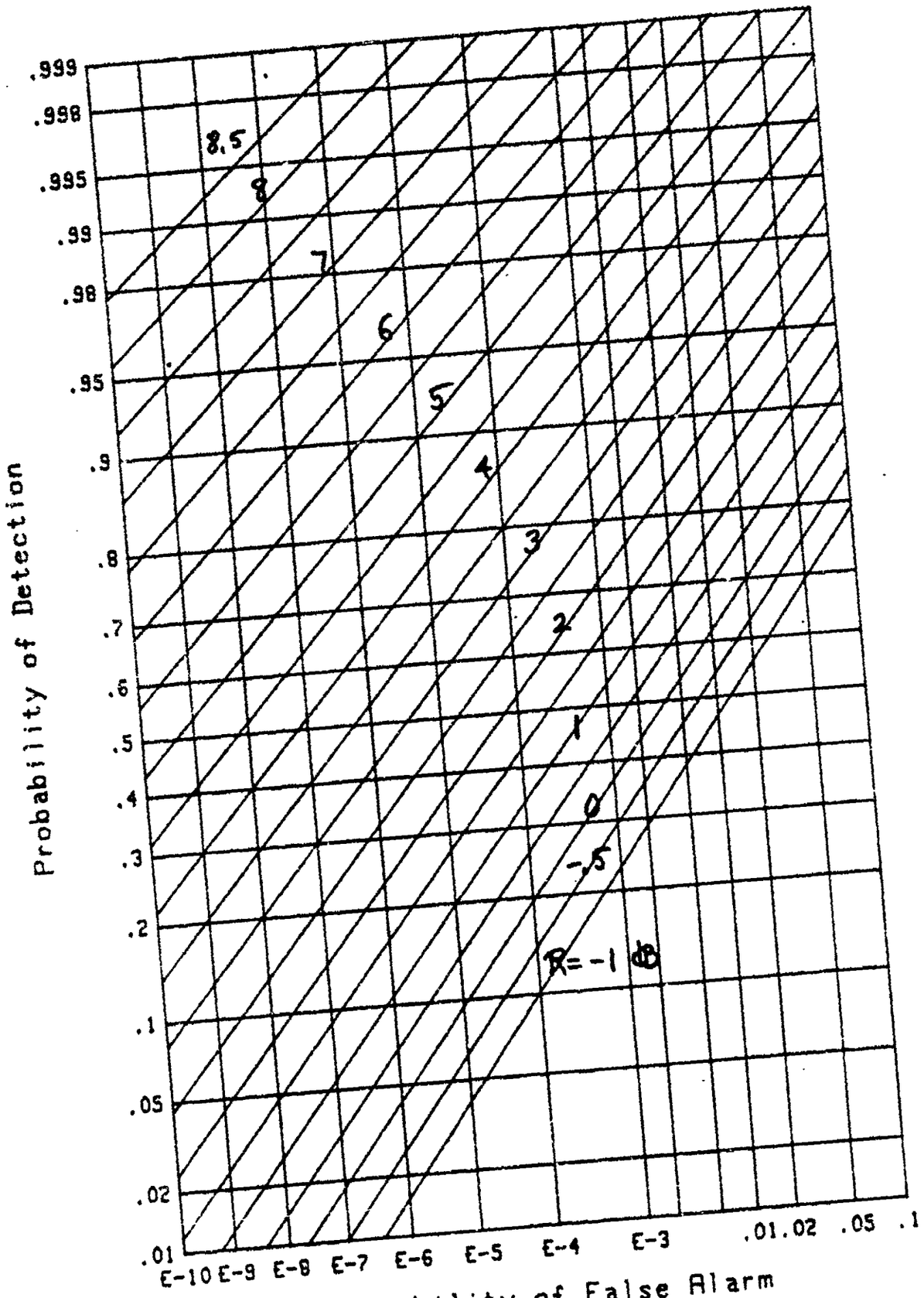

Figure 15. ROC for M=16, Random Weights

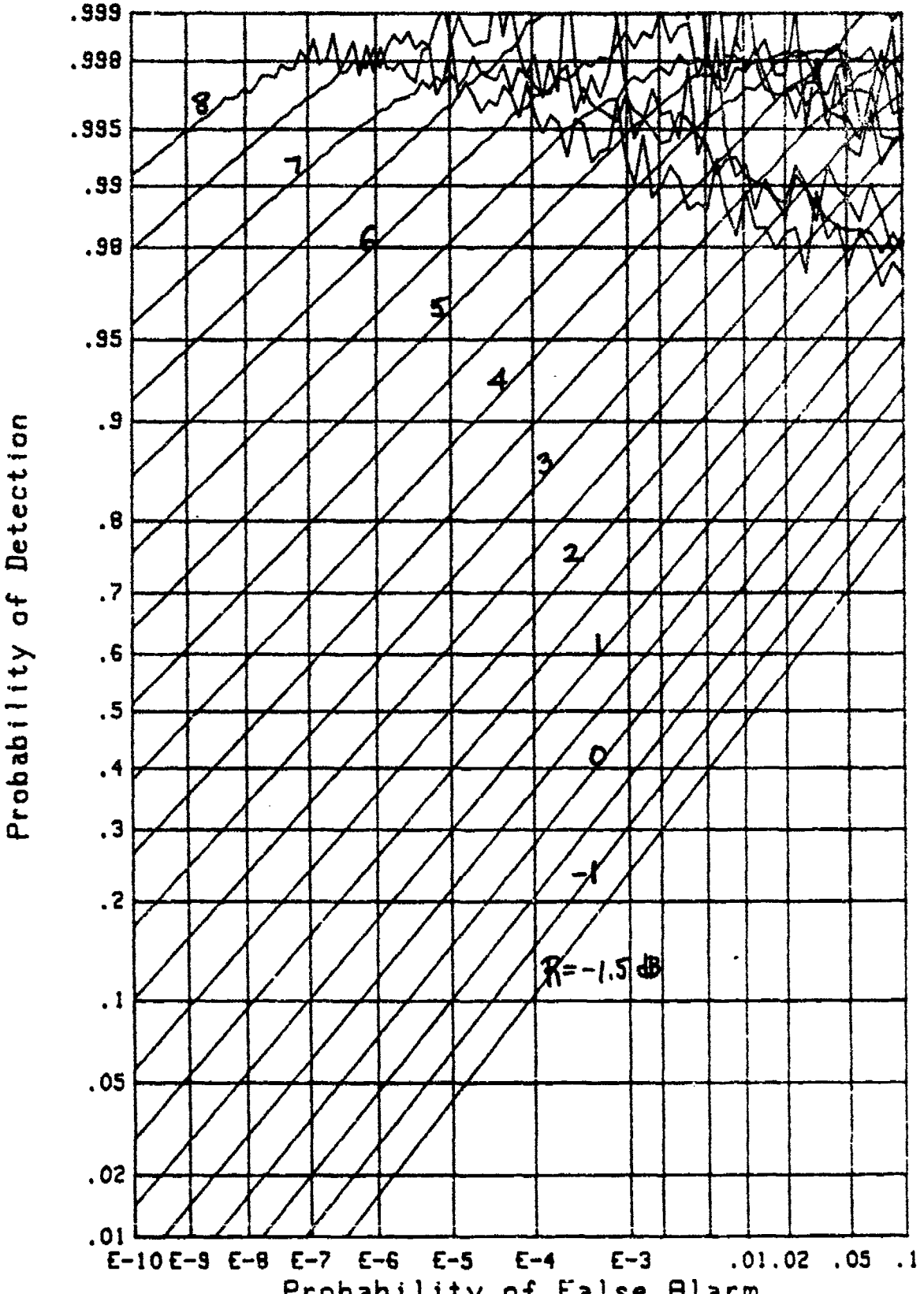

Figure 16. ROC for M=20, Random Weights

CHI-SQUARED APPROXIMATION FOR ARBITRARY WEIGHTS

The difficulty of evaluating the ROC from exact characteristic functions of the form of (7) and (10) has prompted the use of approximations that attempt to extract an effective number of independent samples from a general weight structure, and use this parameter in a simpler chi-squared fit. For example, in [6; (38) and sequel], such an approximation was fruitfully employed to study the stability of a spectral analysis technique employing equi-weighted overlapped segments. Also, in [9; (A-24) - (A-28)], a chi-squared approximation was adopted for the analysis of a diversity combiner in a partially-correlated fading channel. However, in this latter case, no quantitative measure of the error in the approximation was given.

PARAMETERS OF APPROXIMATION

Here, we will address the adequacy of the chi-squared approximation for a general exponential weight structure of the form of (27). We begin by generalizing the chi-squared characteristic function in (12) to the candidate form

$$f_e(\xi) = (1 - i\xi w_e a)^{-M_e} , \qquad (28)$$

where w_e is an effective weight and M_e is an effective number of envelope-squared samples, which may be noninteger. (The number of degrees of freedom in (28) is $2M_e$.) The corresponding probability density and exceedance distribution functions are

$$p_e(u) = \frac{u^{M_e-1} \exp\left(\frac{-u}{w_e a}\right)}{\Gamma(M_e)\,(w_e a)^{M_e}} \qquad \text{for} \quad u > 0 \ ,$$

$$Q_e(u) = \Gamma\left(M_e, \frac{u}{w_e a}\right) \Big/ \Gamma(M_e) \qquad \text{for} \quad u > 0 \ , \tag{29}$$

respectively, where $\Gamma(\cdot,\cdot)$ is the incomplete gamma function [10; 6.5.3]. These results generalize (13) and (14). The (scaled) cumulants of this gamma distribution follow from (28) as

$$\frac{1}{(k-1)!}\, \chi_e(k) = M_e\, (w_e a)^k \quad \text{for } k \geq 1 \ . \tag{30}$$

The mean and variance of this approximation are therefore $M_e\, w_e\, a$ and $M_e\, w_e^2\, a^2$, respectively.

When we equate these first two moments of the generalized chi-squared approximation (28) to the first two moments of decision variable x in (9) and (8), we find

$$w_e = \frac{W_2}{W_1} \ , \qquad M_e = \frac{W_1^2}{W_2} = \frac{\left(\sum_{m=1}^{M} w_m\right)^2}{\sum_{m=1}^{M} w_m^2} \ . \tag{31}$$

For example, if all the weights are equal, then $M_e = M$. On the other hand, if all the weights are zero except for one, then $M_e = 1$. Both of these limiting cases obviously agree with physical intuition. Observe that w_e and M_e are independent of parameter a or R, the signal-to-noise ratio.

For the exponential weight structure in (27), the effective number of weights and the effective weight are

$$M_e = \frac{1 + r}{1 - r} \frac{1 - r^M}{1 + r^M}, \quad w_e = \frac{1}{M_e} \quad \text{for } W_1 = 1 . \tag{32}$$

It should be noted that as $M \to \infty$, effective number M_e saturates at value $(1 + r)/(1 - r)$, which is not infinite.

Since the incomplete gamma function in (29) is tedious to compute for M_e noninteger, performance could be bracketed by the two cases M_i, M_i+1, where M_i is the integer part of M_e. Or interpolation could be used between these two cases. Instead, we shall choose examples for which M_e is an integer; this allows us to use a form like (14), which is easily computed upon replacement of M by M_e.

GRAPHICAL RESULTS

The first example of the use of a chi-squared approximation, for the exponential weight structure in (27), is furnished by figure 17 for $M = 5$, $r = .69308907$; this particular r value is chosen to yield $M_e = 4$, as may be verified from (32). The exact results (solid lines) in this figure were obtained by the method of the previous section, namely, all weights different. The three dashed curves are yielded by the chi-squared approximation of this section, with $M_e = 4$; the latter are seen to be optimistic by almost 1 dB along the left edge of the figure.

When M is increased to 25 and r decreased to .60000182, again resulting in $M_e = 4$, figure 18 shows that the chi-squared approximation is far worse. The reason for this behavior is that

25 significantly different weights cannot be well represented by 4 equal weights in terms of evaluating the detection capability of the energy detector (1).

The series of plots in figures 19, 20, 21, 22, 23 correspond, respectively, to M_e = 8, 16, 32, 64, 128, for various combinations of M and r, as indicated on the figures. Again, the chi-squared approximation is generally optimistic in the useful range of performance. For M = 64 in figure 20, the discrepancy is almost 1 dB along the left edge. However, for large M, like 200 in figure 23, the difference is only about .25 dB along the left edge.

The results in figures 21, 22, 23 for M_e = 32, 64, 128, respectively, were not obtainable from the all-weights-different method of the previous section, due to excessively large coefficients $\{B_m\}$ in (22). Instead, it was necessary to resort to the numerical integration procedure given in [2]; the values of increment Δ_ξ and length L_ξ appropriate to each case are indicated on each figure.

A conclusion to be drawn from the results in this section is that, although the chi-squared approximation is much better than the Gaussian approximation, it is still not adequate for accurate performance predictions within a few tenths of a decibel. The chi-squared approximation is generally unacceptable for small M_e, unless r is very close to 1. And for large M_e, it is acceptable in some regions of the ROC, but not in others, especially if the extreme weight ratio, r^{M-1}, is very small.

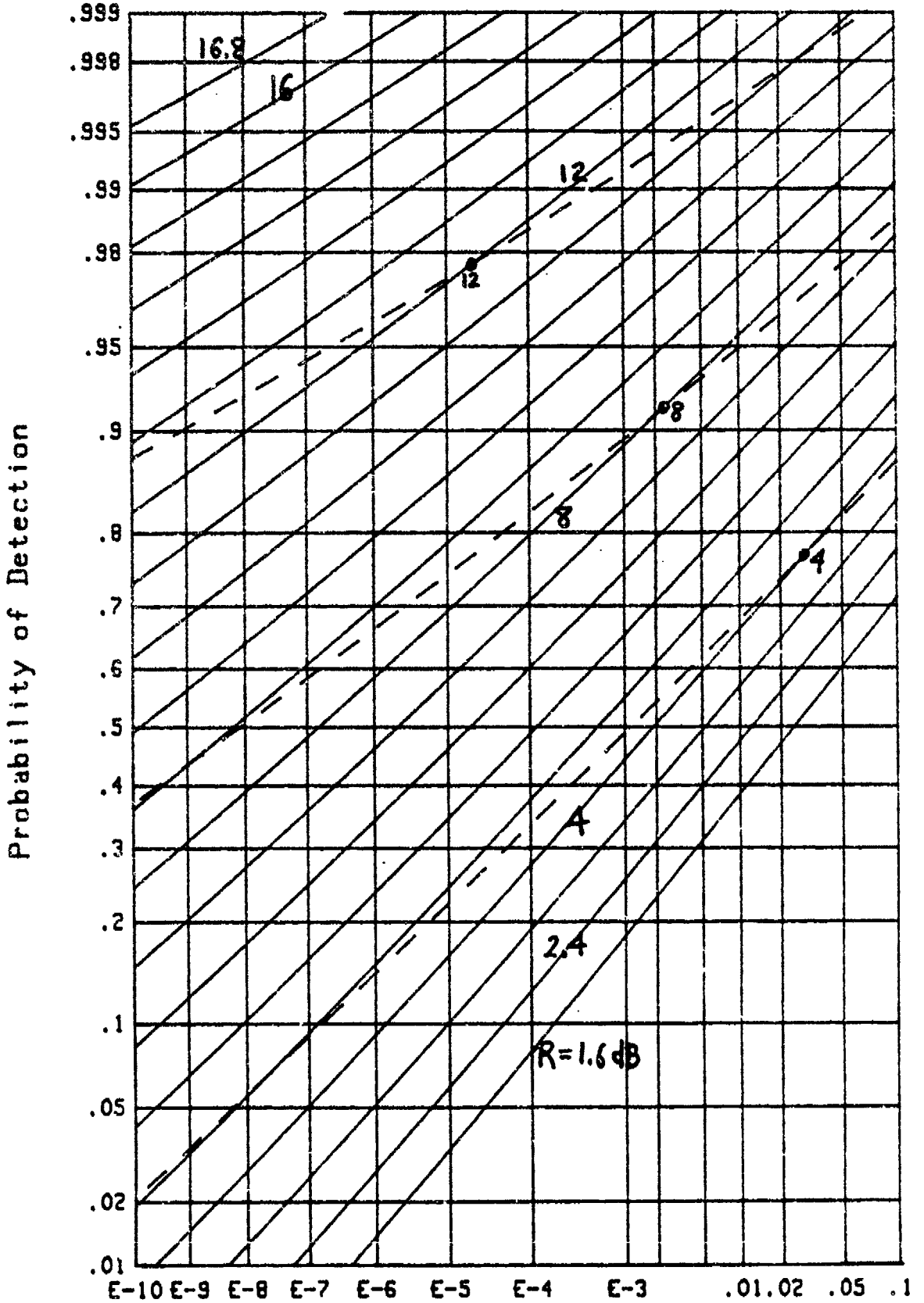

Figure 17. ROC for M=5, r=.69388907 (M_e=4)

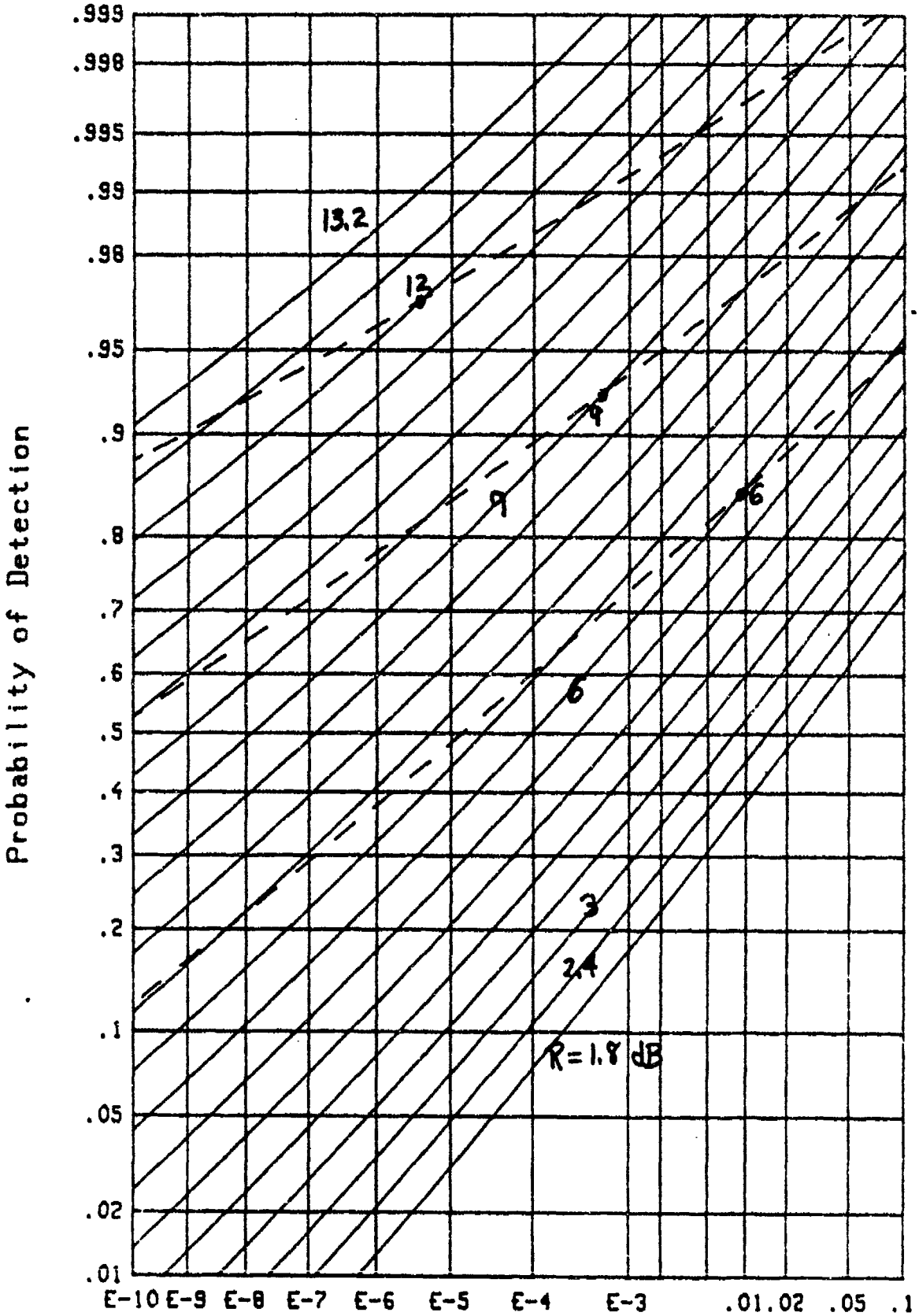

Figure 18. ROC for M=25, r=.60000182 (M_e=4)

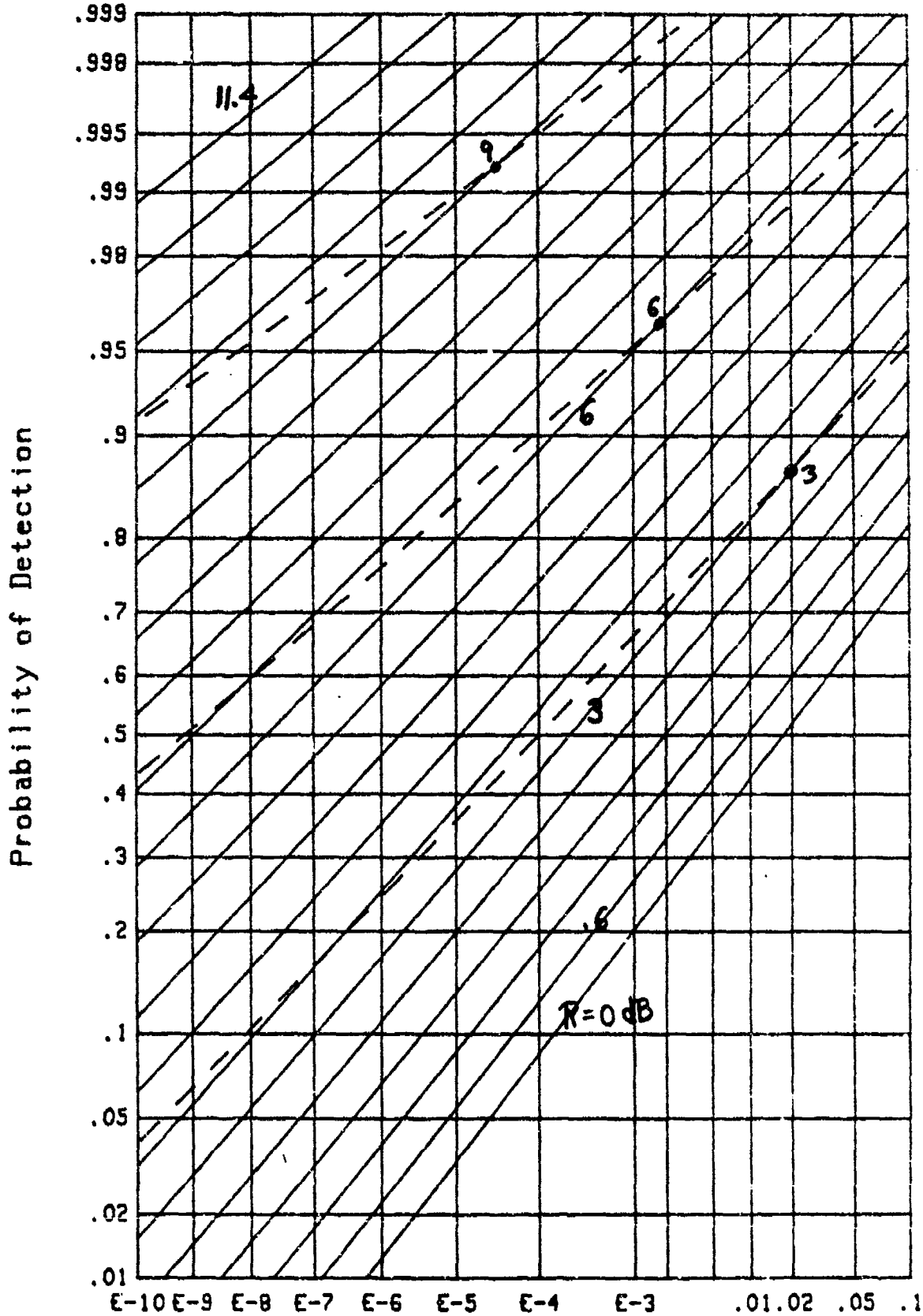

Figure 19. ROC for M=10, r=.83623826 (M_e=8)

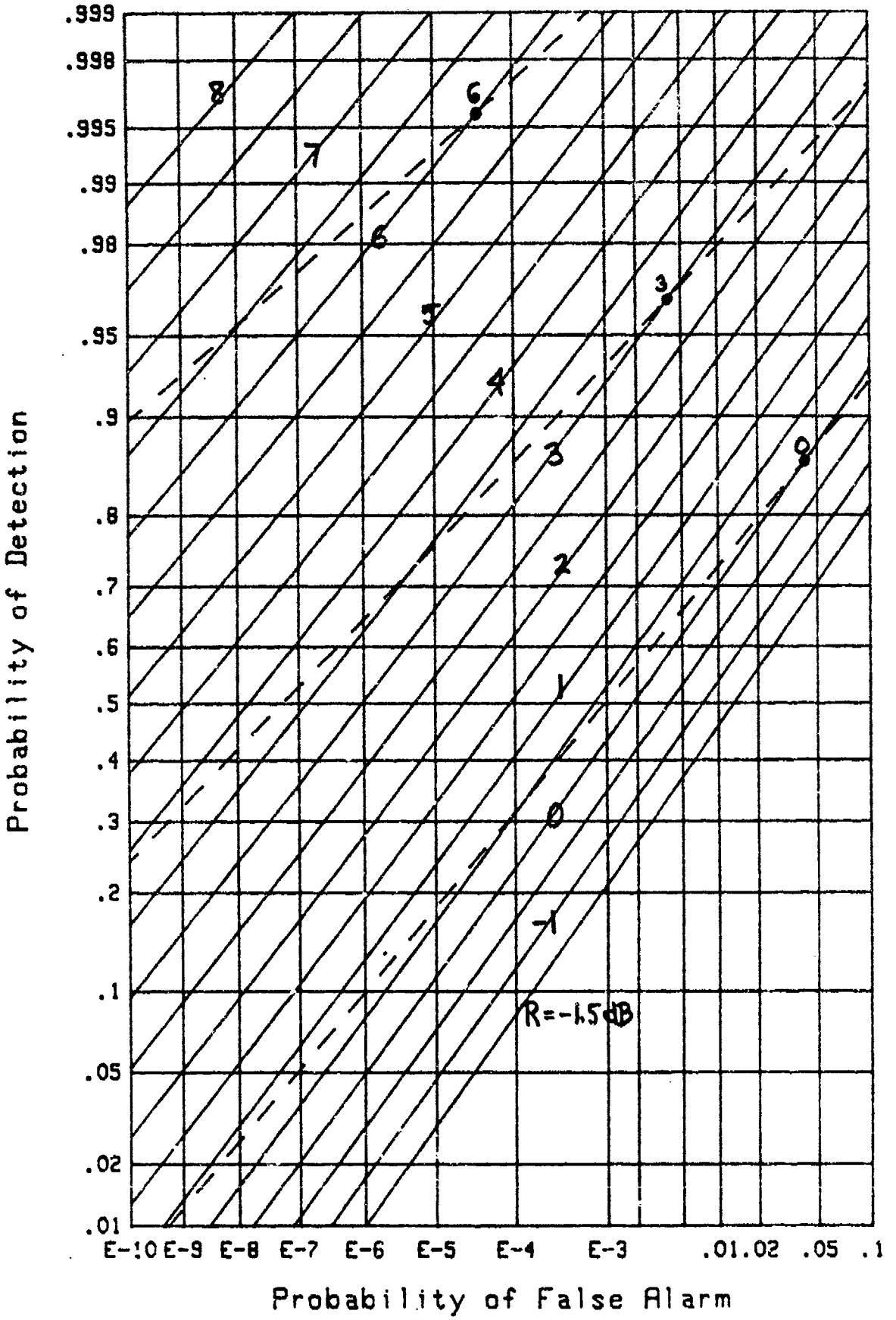

Figure 20. ROC for M=64, r=.88242683 (M_e=16)

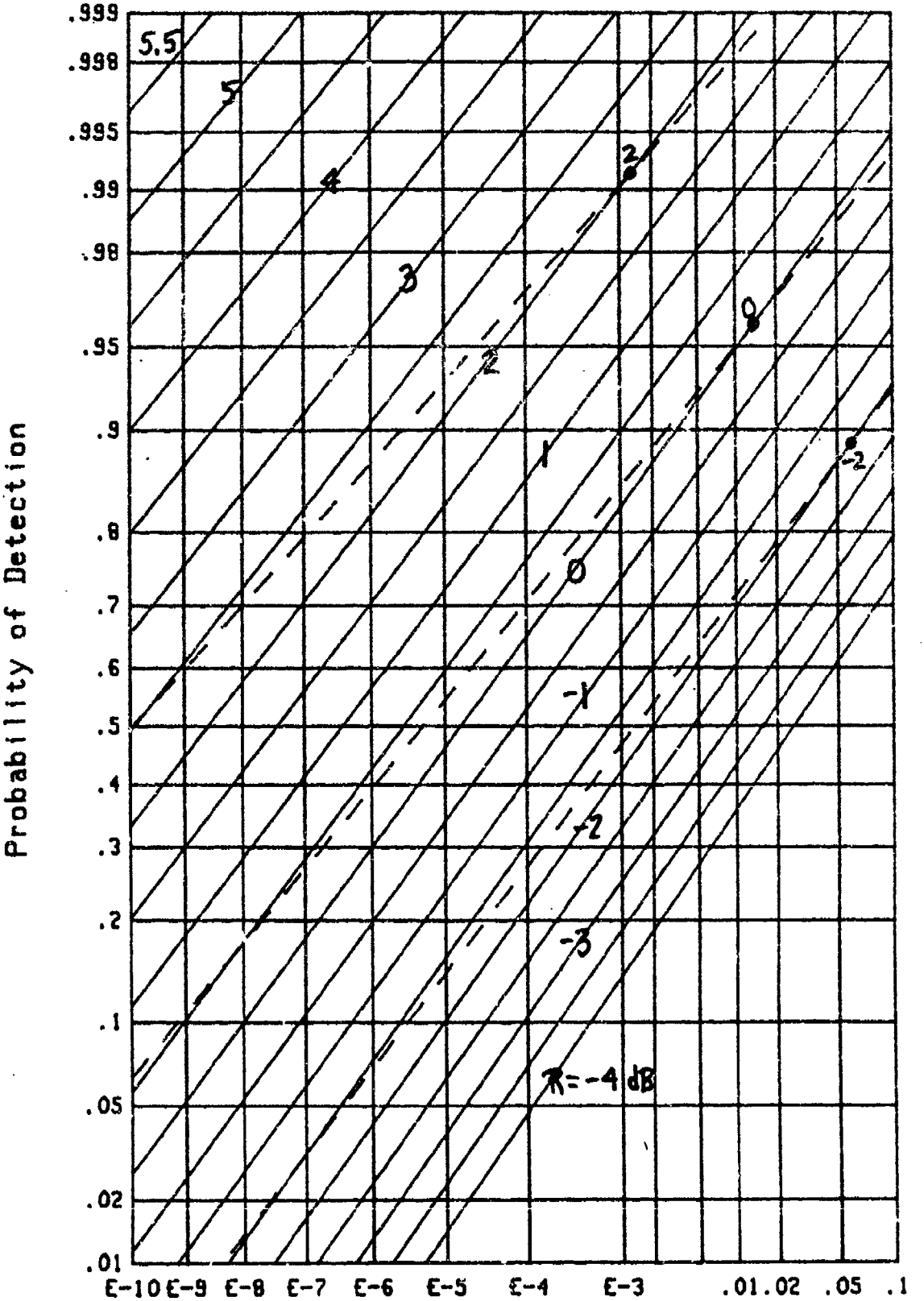

Figure 21. ROC for M=50, r=.94648071 (M_e=32)

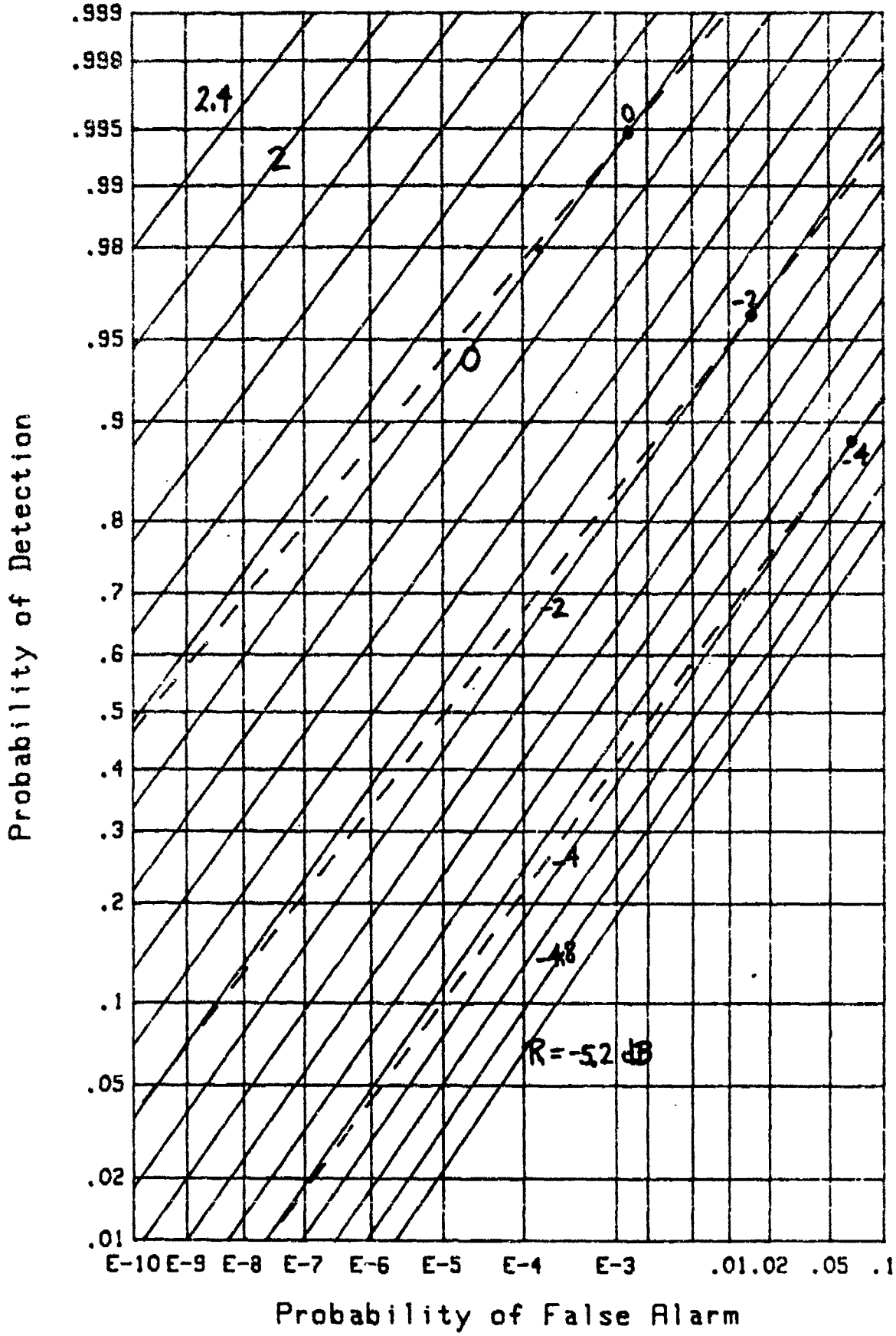

Figure 22. ROC for M=100, r=.97288022 (M_e=64)

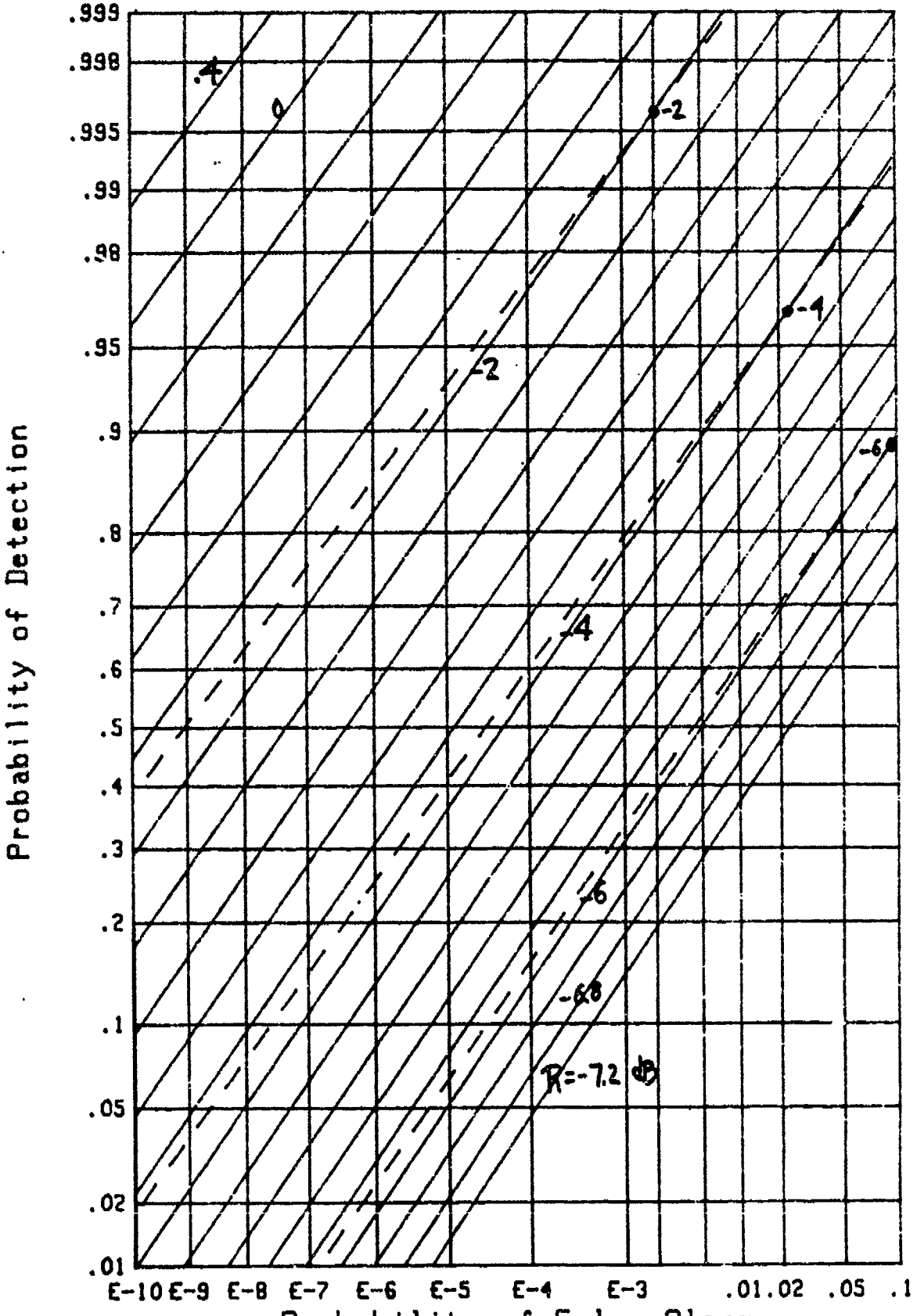

Figure 23. ROC for M=200, r=.98634790 (M_e=128)

THIRD-ORDER APPROXIMATION FOR ARBITRARY WEIGHTS

When a constant c is added to a random variable, the characteristic function is modified by multiplication by the factor $\exp(ic\xi)$. Accordingly, a further generalization of the chi-squared characteristic function in (28) is afforded by

$$f_c(\xi) \equiv \frac{\exp(i\xi b_c a)}{(1 - i\xi w_c a)^{M_c}} = \exp\left(i\xi b_c a - M_c \ln(1 - i\xi w_c a)\right) . \quad (33)$$

This form now has three parameters to choose, namely w_c, b_c, and effective number of samples M_c. This is in distinction to the chi-squared approximation (28) and the Gaussian approximation (A-2), both of which had only two free parameters to adjust. Thus, whereas we only matched the first two moments in (30) and (A-3), respectively, to those of decision variable x, we can now match the first <u>three</u> moments of x if we use characteristic function model (33).

The cumulants of characteristic function (33) are

$$\chi_c(1) = M_c w_c a + b_c a ,$$

$$\frac{1}{(k-1)!} \chi_c(k) = M_c (w_c a)^k \quad \text{for } k \geq 2 . \quad (34)$$

When the first three cumulants (or moments) of (34) are equated with the corresponding quantities of decision variable x, as given by (8), the unique solutions for the parameters of (33) are

$$M_c = \frac{W_2^3}{W_3^2} , \quad w_c = \frac{W_3}{W_2} , \quad b_c = W_1 - \frac{W_2^2}{W_3} , \quad (35)$$

where

$$W_k = \sum_{m=1}^{M} w_m^k \ . \tag{36}$$

It should be noted that the parameters in (35) are independent of parameter a or R, the signal-to-noise ratio.

The probability density function corresponding to characteristic function (33) is

$$p_c(u) = \frac{(u - b_c a)^{M_c - 1} \exp\left(\frac{-u + b_c a}{w_c a}\right)}{\Gamma(M_c)\ (w_c a)^{M_c}} \quad \text{for} \quad u > b_c a \ , \tag{37}$$

and zero otherwise. The exceedance (gamma) distribution function is an obvious generalization of (29), or (14) if M_c is integer; see [10; 6.5.3, 6.5.2, 6.5.13].

$$Q_c(u) = \Gamma\left(M_c, \frac{u - b_c a}{w_c a}\right) \Big/ \Gamma(M_c) = E_{M_c - 1}\left(\frac{u - b_c a}{w_c a}\right) \text{ for } u > b_c a \ . \tag{38}$$

For threshold value T, the false alarm and detection probabilities follow immediately as

$$P_F = E_{M_c - 1}\left(\frac{T - b_c}{w_c}\right) \ , \quad P_D = E_{M_c - 1}\left(\frac{T - b_c a}{w_c a}\right) \ , \tag{39}$$

provided that $T > b_c a$.

EXPONENTIAL WEIGHTS

We now restrict attention to the exponential weight structure

$$w_m = \frac{1 - r}{1 - t} r^{m-1} \quad \text{for} \quad 1 \le m \le M , \quad \text{with } t = r^M , \qquad (40)$$

where we have normalized at $W_1 = 1$. Then, from (36),

$$W_k = \left(\frac{1 - r}{1 - t}\right)^k \frac{1 - t^k}{1 - r^k} = \left(\frac{1 - r}{1 - t}\right)^{k-1} \frac{1 + t + t^2 + \cdots + t^{k-1}}{1 + r + r^2 + \cdots + r^{k-1}} . \qquad (41)$$

In particular,

$$W_1 = 1 , \quad W_2 = \frac{1 - r}{1 - t} \frac{1 + t}{1 + r} , \quad W_3 = \left(\frac{1 - r}{1 - t}\right)^2 \frac{1 + t + t^2}{1 + r + r^2} . \qquad (42)$$

The parameters in (35) then follow by substitution as

$$M_c = \frac{(1 - r^3)^2}{(1 - r^2)^3} \frac{(1 - t^2)^3}{(1 - t^3)^2} = \frac{1 - t}{1 - r} \left(\frac{1 + t}{1 + r}\right)^3 \left(\frac{1 + r + r^2}{1 + t + t^2}\right)^2 , \qquad (43)$$

$$w_c = \frac{1 - r^2}{1 - t^2} \frac{1 + t + t^2}{1 + r + r^2} ; \quad b_c = \frac{(1 - r\,t)\,(r - t)}{(1 + r)^2\,(1 + t + t^2)} . \qquad (44)$$

For equal weights, $w_m = 1/M$, we get the usual reduction to $W_1 = 1$, $W_2 = 1/M$, $W_3 = 1/M^2$, giving $M_c = M$, $w_c = 1/M$, $b_c = 0$. Furthermore, it is shown in appendix B that additive constant b_c in (33) and (37), as determined from (35) and (36), is never negative, for <u>any</u> nonnegative weight structure $\{w_m\}$.

GRAPHICAL RESULTS

The first example we consider here is M = 25, r = .75049209, for which (43) gives $M_c = 4$; again, the reason for the particular choice of r is made so that M_c is integer and (39) can be used. The approximation afforded by (39) is superposed (dashed lines) in figure 24 on the exact results (solid lines) obtained from (25). Increasing M to 64 and changing r to .75049170, so that M_c is maintained at 4, generates virtually the same approximation. The fit is poor and rather optimistic at the left edge of the figure, due to the small value of M_c, namely 4.

For M = 50 and r = .96915298, M_c is increased to 32 and the results are compared in figure 25. Now, the fit afforded by the constant plus chi-squared approximation is rather good over the entire range of false alarm and detection probabilities shown; in fact, the approximation is optimistic by about .1 dB on the left edge of the figure. The reason for this development is the larger value of the effective number of samples, M_c, namely 32.

Two more results, for M_c equal to 64 and 128, yield similar conclusions in figures 26 and 27, respectively. Again, the exponential weight structure was employed. However, the goodness of fit of the constant plus chi-squared approximation is not limited to this type of weights, but in fact applies to arbitrary structures. To back up this statement, an example of uniformly distributed random weights for M = 133 and $M_c = 77.971$ is displayed in figure 28; the overlay, which used $M_c = 78$ in approximation (39), is seen to be very good for this value of M_c.

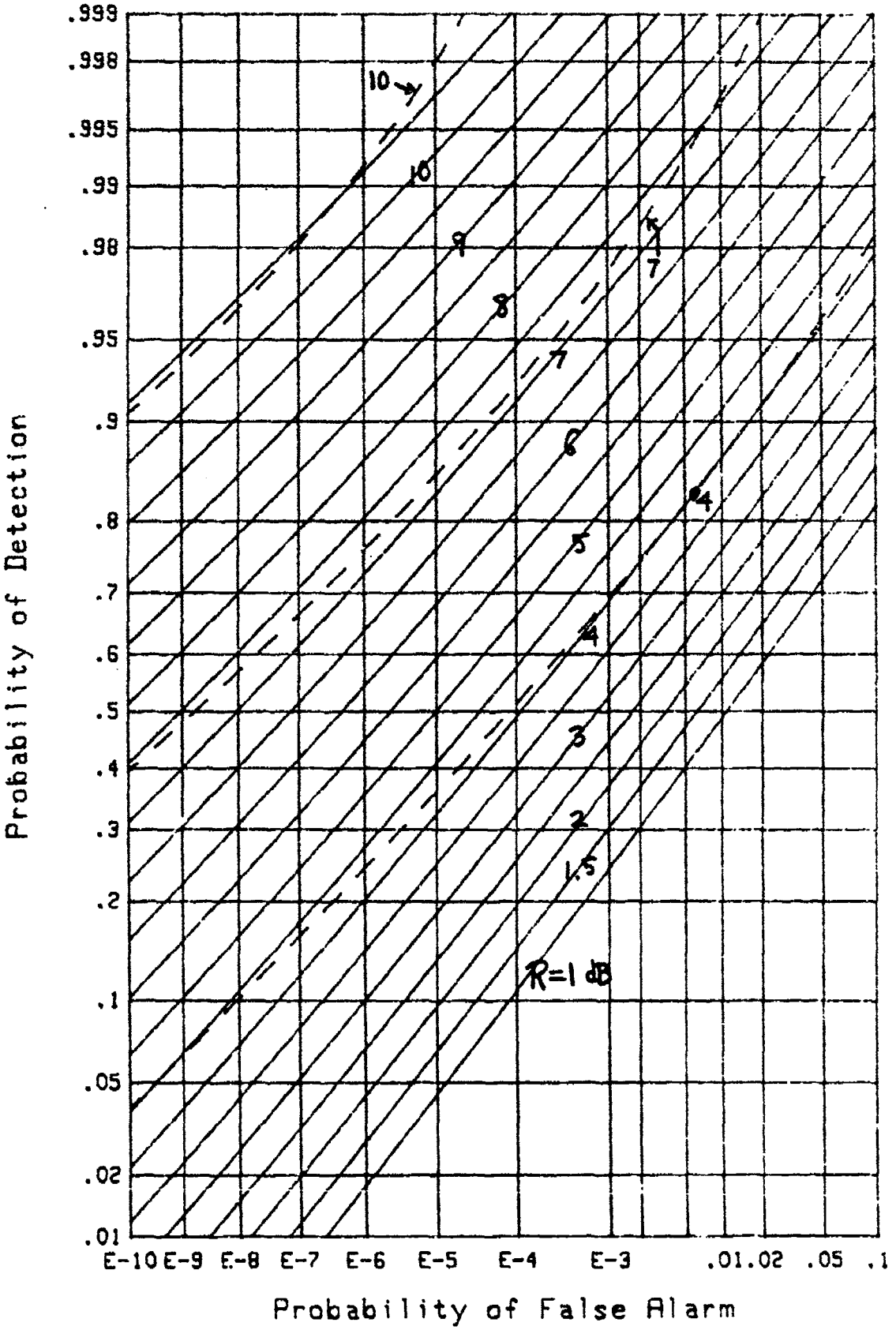

Figure 24. ROC for M=25, r=.75049209 (M_c=4)

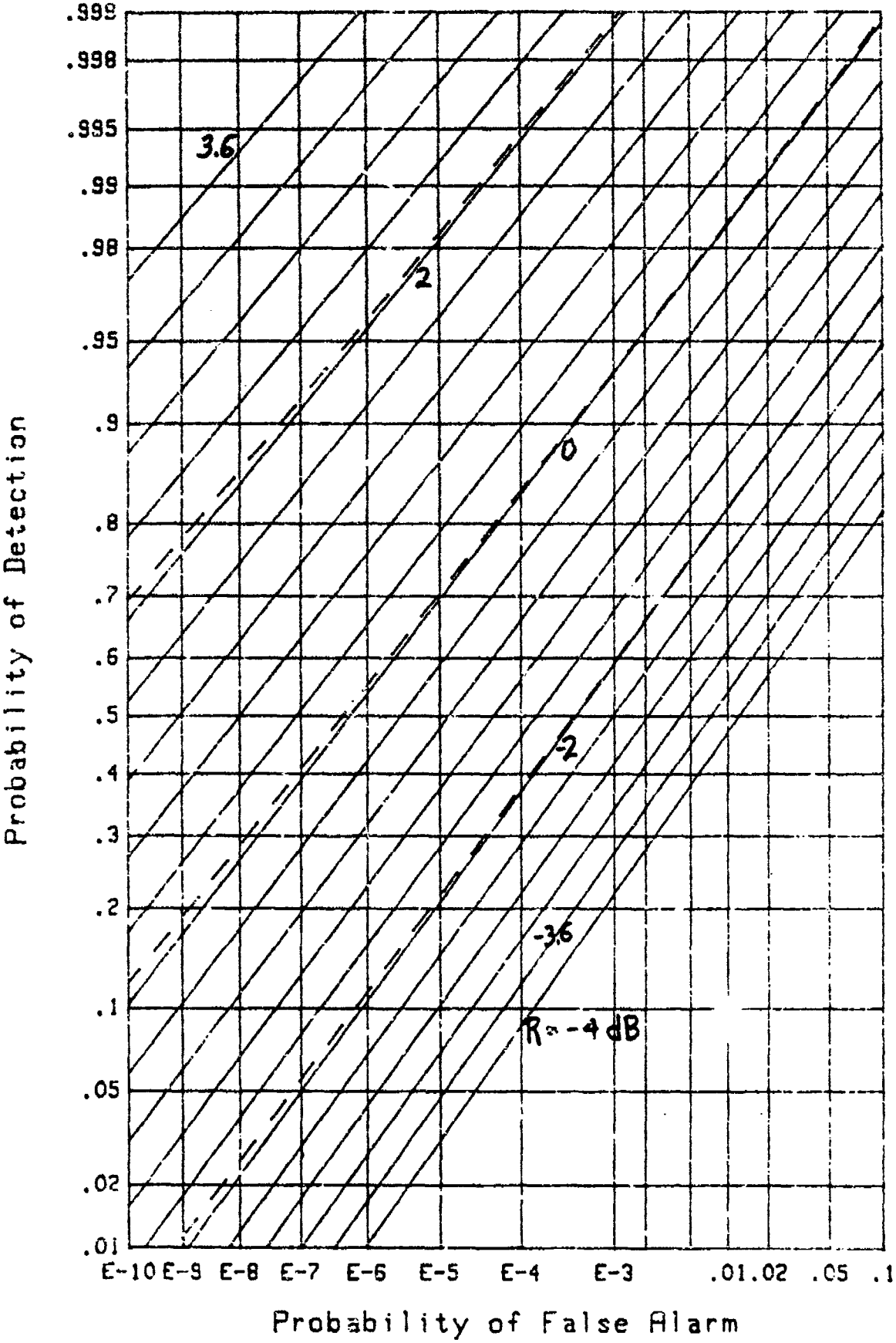

Figure 25. ROC for M=50, r=.96915298 (M_c=32)

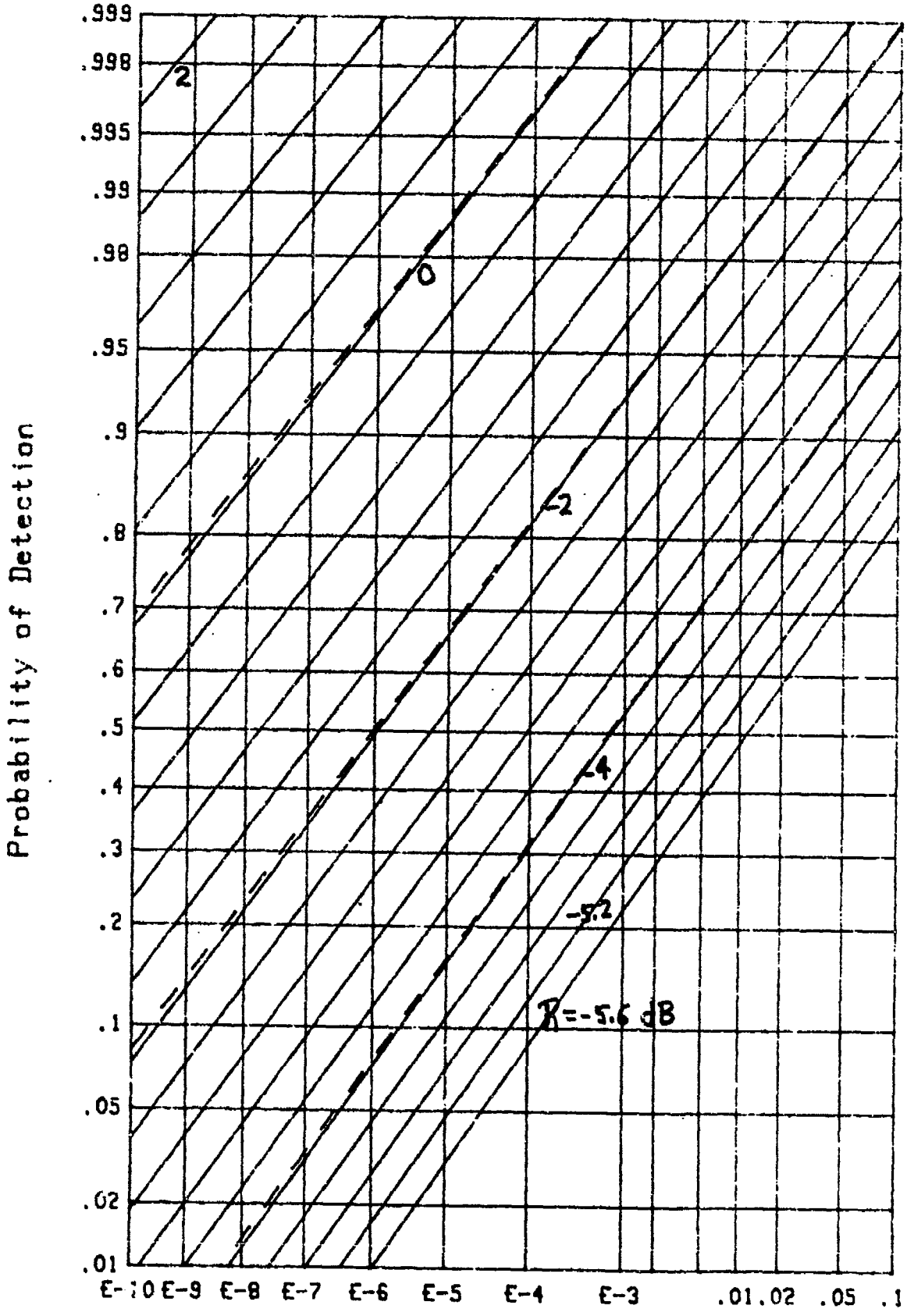

Figure 26. ROC for M=100, r=.98445999 (M_c=64)

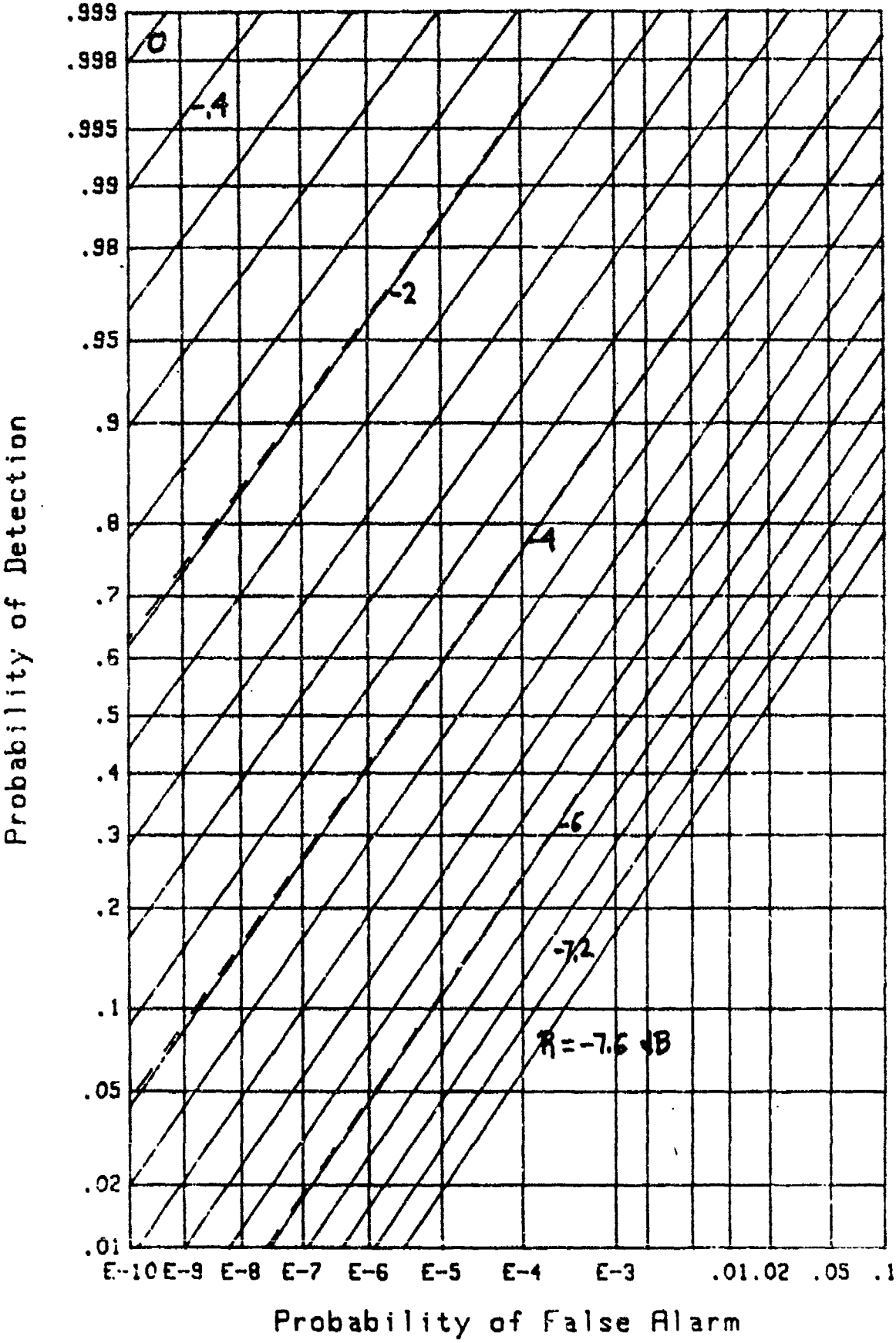

Figure 27. ROC for M=200, r=.99220012 (M_c=128)

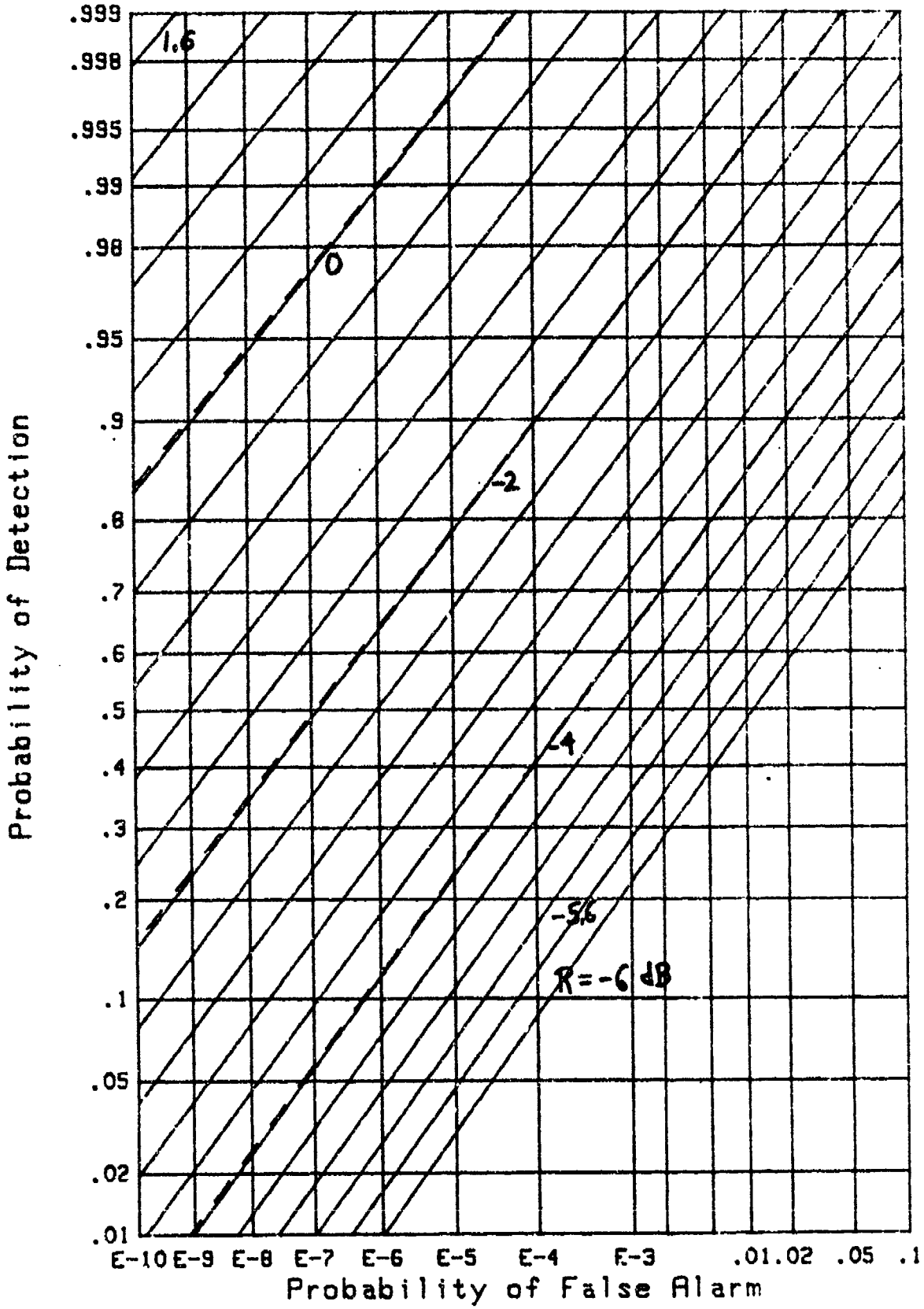

Figure 28. ROC for M=133, Random Weights (M_c=78)

APPLICATION TO EIGENVALUE PROBLEM

Earlier, in (10) and [8; (24)], a particular characteristic function was given which has occurred in a number of statistical analyses. That characteristic function, in normalized form, is

$$f_x(\xi) = \left[\prod_{m=1}^{M}\left\{1 - i\xi\left(1 + R\,\lambda_m\right)\right\}\right]^{-1} , \qquad (45)$$

where R is the per-sample signal-to-noise ratio and $\{\lambda_m\}$ are the eigenvalues of the normalized covariance matrix P of the fading signal components. By expanding the ln of (45) in a power series in $i\xi$, the cumulants of random variable x are found to be

$$\frac{1}{(k-1)!}\,\chi_x(k) = \sum_{m=1}^{M}(1 + R\,\lambda_m)^k = \sum_{m=1}^{M}\sum_{n=0}^{k}\binom{k}{n} R^n\,\lambda_m^n =$$

$$= M + \sum_{n=1}^{k}\binom{k}{n} R^n\,\mathrm{tr}\left(P^n\right) \quad \text{for } k \geq 1 , \qquad (46)$$

where we have used the simplifying result in appendix C regarding sums of powers of eigenvalues. In particular, there follows from (46), the first three cumulants of x in terms of $\mathrm{tr}(P^n)$:

$$\chi_x(1) = M + R\,\mathrm{tr}(P) ,$$

$$\chi_x(2) = M + 2R\,\mathrm{tr}(P) + R^2\,\mathrm{tr}(P^2) ,$$

$$\tfrac{1}{2}\chi_x(3) = M + 3R\,\mathrm{tr}(P) + 3R^2\,\mathrm{tr}(P^2) + R^3\,\mathrm{tr}(P^3) . \qquad (47)$$

PARAMETERS FOR CANDIDATE APPROXIMATION

In this section, we will approximate exact characteristic function (45) by the form employing the constant plus chi-squared idea again, namely

$$f_d(\xi) = \frac{\exp(i\xi b_d)}{(1 - i\xi w_d)^{M_d}} = \exp\left(i\xi b_d - M_d \ln(1 - i\xi w_d)\right) . \quad (48)$$

The cumulants are given by a form very similar to (34), and in particular, the first three (scaled) cumulants of characteristic function (48) are

$$\chi_d(1) = M_d w_d + b_d , \quad \chi_d(2) = M_d w_d^2 , \quad \tfrac{1}{2}\chi_d(3) = M_d w_d^3 . \quad (49)$$

If the first three cumulants, $\chi_d(k)$ for k=1,2,3, were specified, we could then solve (49) for the required parameters according to

$$M_d = \frac{\chi_d^3(2)}{\left(\chi_d(3)/2\right)^2} , \quad w_d = \frac{\chi_d(3)/2}{\chi_d(2)} , \quad b_d = \chi_d(1) - \frac{\chi_d^2(2)}{\chi_d(3)/2} . \quad (50)$$

Now, we set the cumulants of approximation (48) equal to the exact cumulants given by (47), and then solve (50) for the required parameter values. Then, approximation (48) to exact characteristic function (45) is available for numerical evaluation. If cumulants $\{\chi_x(k)\}$ for k=1,2,3 can be evaluated either analytically (via eigenvalues $\{\lambda_m\}$ in (46) or by the trace relations in (47)) or numerically (estimated via finite time averages), then the parameters in (50) can be determined and the corresponding ROC found.

EXACT PERFORMANCE OF (45)

If signal-to-noise ratio R = 0 in (45), then $f_x(\xi) = (1 - i\xi)^{-M}$ and there follows, in a manner similar to (14), $Q_x(u) = E_{M-1}(u)$ and $P_F = E_{M-1}(T)$ for threshold T.

If R > 0 and <u>all</u> the eigenvalues $\{\lambda_m\}$ in (45) are distinct, then, in a manner similar to (21), we can express

$$f_x(\xi) = \sum_{m=1}^{M} \frac{B_m(R)}{1 - i\xi\left(1 + R\ \lambda_m\right)} , \tag{51}$$

where coefficients

$$B_m(R) = \frac{\left(1 + R\ \lambda_m\right)^{M-1}}{R^{M-1} \prod_{\substack{k=1 \\ k \neq m}}^{M} \left(\lambda_m - \lambda_k\right)} \quad \text{for } 1 \leq m \leq M . \tag{52}$$

The exceedance distribution function is then

$$Q_x(u) = \sum_{m=1}^{M} B_m(R) \exp\left(\frac{-u}{1 + R\ \lambda_m}\right) \quad \text{for } u > 0 , \quad R > 0 , \tag{53}$$

and the detection probability is

$$P_D = \sum_{m=1}^{M} B_m(R) \exp\left(\frac{-T}{1 + R\ \lambda_m}\right) \quad \text{for } T > 0 , \quad R > 0 . \tag{54}$$

The eigenvalues $\{\lambda_m\}$ of normalized covariance matrix P are independent of signal-to-noise ratio R; however, coefficients $\{B_m(R)\}$ are dependent on R and explicitly indicated so.

GRAPHICAL RESULTS

The only example that we consider here is a covariance matrix $P = [\rho_{mn}]$, where $\rho_{mn} = \rho^{|m-n|}$. In particular, for $M = 10$ and $\rho = .5$, the M eigenvalues $\{\lambda_m\}$ of P were evaluated and the results on page 55 were used for an exact evaluation of the detection and false alarm probabilities; these are displayed as solid lines in figure 29.

Then, we returned to matrix P, ignored the knowledge of the eigenvalues, and instead employed the trace relations in (47) and appendix C to evaluate the cumulants of random variable x. These were substituted in (50) to determine the parameters of characteristic function (48), as explained in the sequel to (50). Then, the method of [2] was used to obtain the corresponding ROC.

These results are overlaid as dashed lines in figure 29, for three selected values of signal-to-noise ratio R (in decibels). The agreement for small signal-to-noise ratios is very good, and can be explained by observing that (45) approaches the chi-squared characteristic function in this case. Approximation (48) is also excellent for very small false alarm probabilities, despite the fact that the equivalent number of samples, M_d, is rather small; for example, the three curves in figure 29 for $R = 2,5,8$ dB have $M_d = 5.79, 4.83, 4.31$, respectively.

Another example for $M = 32$, $\rho = .5$ is displayed in figure 30. Here, the values of M_d for the four overlays, $R = -2,0,2,4$ dB are 24.1, 20.6, 17.6, 15.4, respectively. These larger values of M_d account for the improved fit to the exact results.

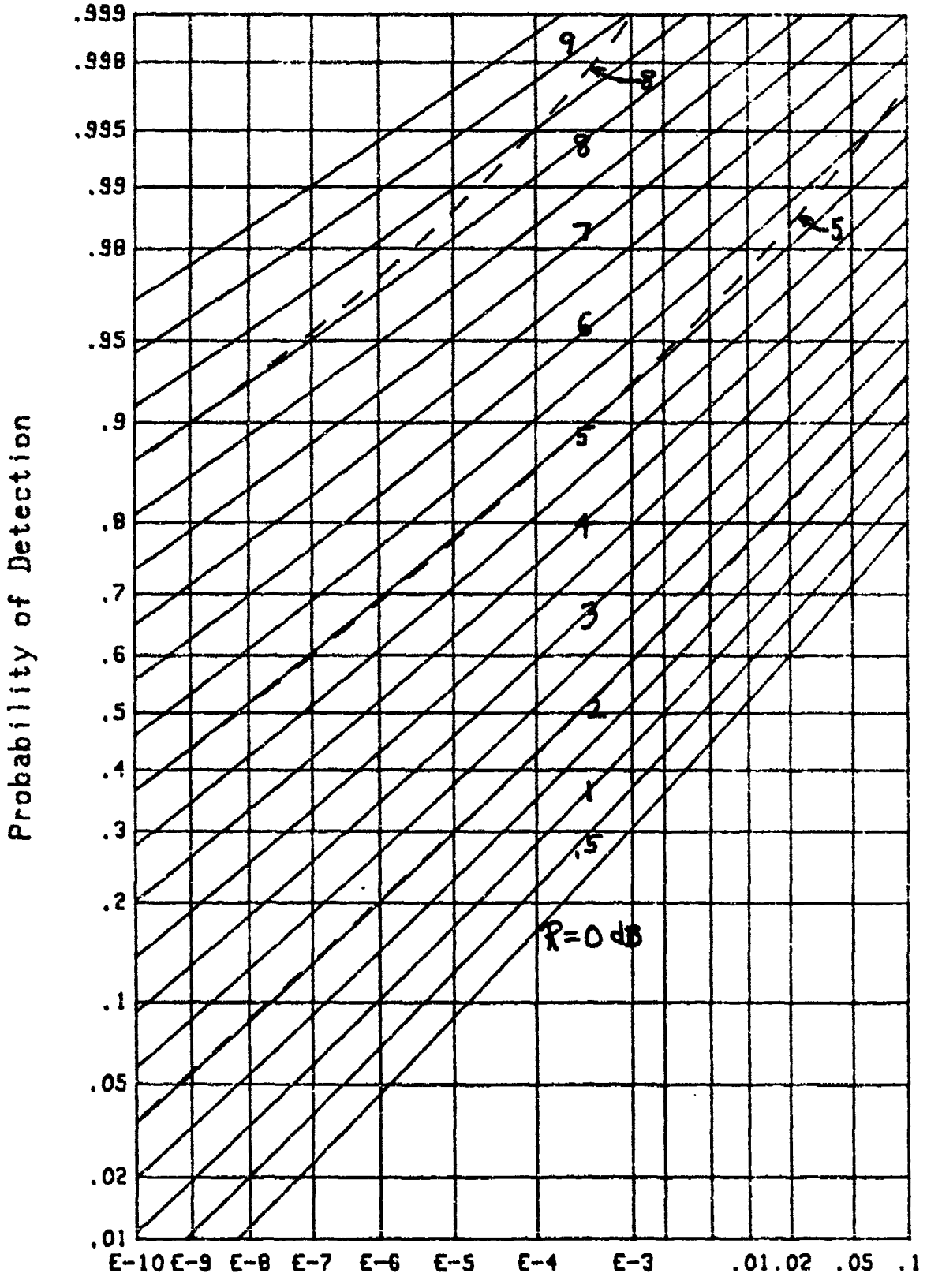

Figure 29. ROC for M=10, ρ=.5

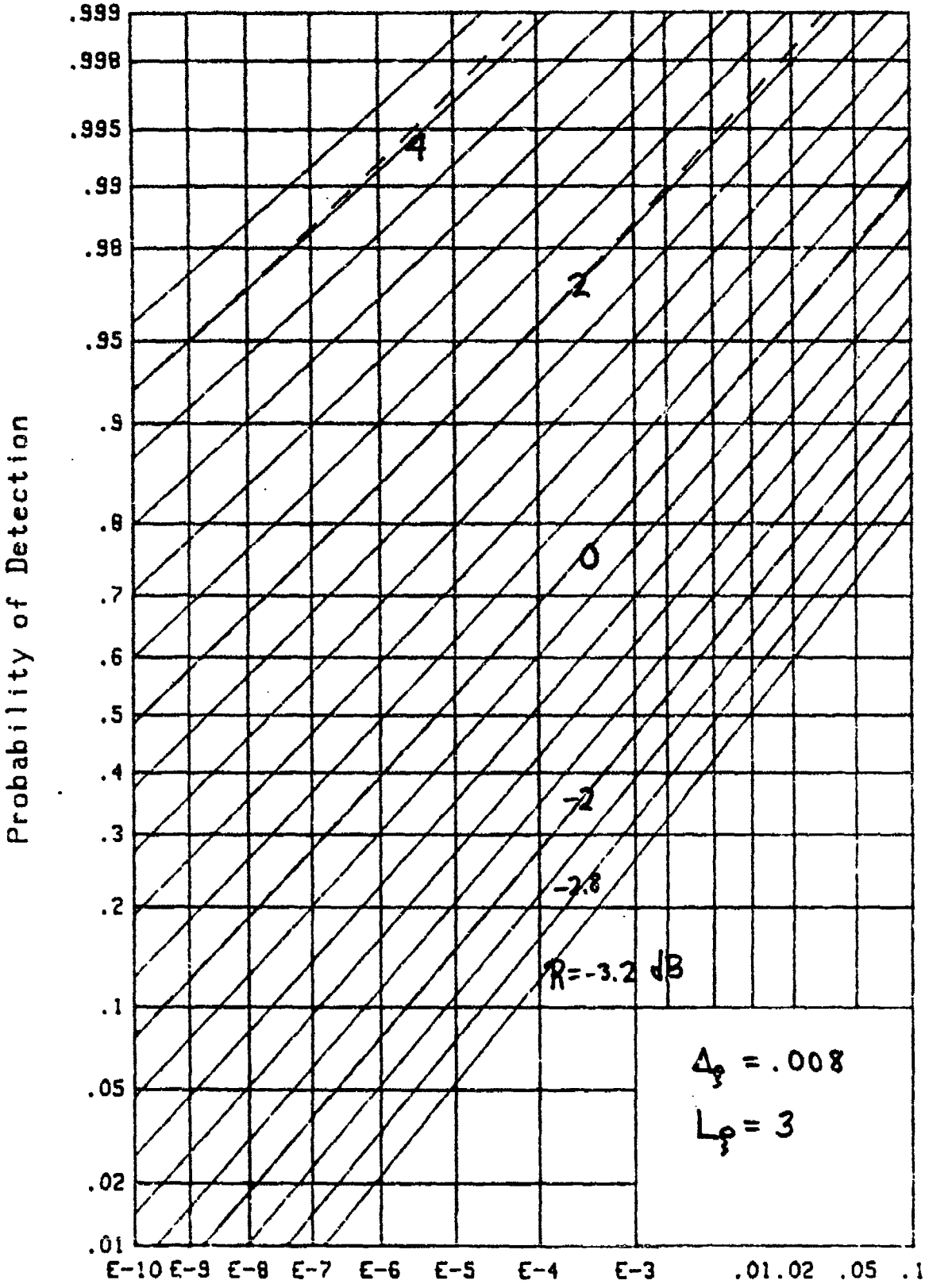

Figure 30. ROC for M=32, ρ=.5

FOURTH-ORDER APPROXIMATIONS FOR ARBITRARY WEIGHTS

In this section, we will consider a couple of fourth-order fits to a specified characteristic function and will match cumulants (or moments) through fourth-order.

GAUSSIAN PLUS CHI-SQUARED FIT

The initial fourth-order fit of interest here corresponds to the characteristic function of a (nonzero mean) Gaussian random variable plus a chi-squared variate. That is, the candidate is

$$f_f(\xi) = \frac{\exp\left(i\xi b_f - \frac{1}{2}\xi^2 c_f\right)}{\left(1 - i\xi w_f\right)^{M_f}} = \exp\left(i\xi b_f - \frac{1}{2}\xi^2 c_f - M_f \ln(1 - i\xi w_f)\right) . \tag{55}$$

The first four cumulants of characteristic function (55) are

$$\chi_f(1) = b_f + M_f w_f , \quad \chi_f(2) = c_f + M_f w_f^2 ,$$

$$\frac{1}{2}\chi_f(3) = M_f w_f^3 , \quad \frac{1}{6}\chi_f(4) = M_f w_f^4 . \tag{56}$$

If the cumulants are specified, the parameters for characteristic function (55) can be determined explicitly as

$$M_f = \frac{\left(\chi_f(3)/2\right)^4}{\left(\chi_f(4)/6\right)^3} , \quad w_f = \frac{\chi_f(4)/6}{\chi_f(3)/2} ,$$

$$b_f = \chi_f(1) - \frac{\left(\chi_f(3)/2\right)^3}{\left(\chi_f(4)/6\right)^2} , \quad c_f = \chi_f(2) - \frac{\left(\chi_f(3)/2\right)^2}{\chi_f(4)/6} . \tag{57}$$

Numerical results will be presented in a later section.

NON-CENTRAL CHI-SQUARED FIT

The other fourth-order fit that we consider corresponds to a generalized non-central chi-squared variate, namely characteristic function

$$f_g(\xi) = \frac{\exp\left(\frac{i\xi b_g}{1 - i\xi c_g}\right)}{\left(1 - i\xi w_g\right)^{M_g}} = \exp\left(\frac{i\xi b_g}{1 - i\xi c_g} - M_g \ln(1 - i\xi w_g)\right) . \quad (58)$$

This is called generalized because we do not force $c_g = w_g$. The ln of (58) can be expanded in a power series in $i\xi$:

$$\ln f_g(\xi) = i\xi b_g \sum_{j=0}^{+\infty} (i\xi c_g)^j + M_g \sum_{k=1}^{+\infty} \frac{1}{k} (i\xi w_g)^k . \quad (59)$$

The first four cumulants of this characteristic function are then

$$\chi_g(1) = b_g + M_g w_g , \quad \chi_g(2) = 2 b_g c_g + M_g w_g^2 ,$$

$$\frac{1}{2}\chi_g(3) = 3 b_g c_g^2 + M_g w_g^3 , \quad \frac{1}{6}\chi_g(4) = 4 b_g c_g^3 + M_g w_g^4 . \quad (60)$$

The inversion of these nonlinear equations, for the parameters in terms of the cumulants, is not possible in closed form, as it was for candidate characteristic function (55). This limitation tends to discourage use of the non-central chi-squared approximation (58). However, in appendix D, an efficient numerical procedure for solving (60) for the required parameters is developed and programmed. Application of this approximation procedure is deferred to a later section.

PERFORMANCE IN STEADY STATE NOISE

Up to this point, the number of samples, M, has been finite, both for signal-present as well as signal-absent; then, the noise output of the exponential integrator, (27) or (40), has not reached steady-state. In this section, the number M of noise samples will be set equal to ∞, thereby allowing the integrator noise output to reach steady state. However, the number, N, of samples containing signal (if present) will remain finite.

This situation arises in practice, for example, when the precise arrival time of the signal is unknown. The use of surplus envelope-squared samples $\{z_m\}$, for $m > N$, does <u>not</u> improve performance, since these particular samples are always noise-only; in fact, these extra samples always degrade performance, the exact amount depending on the relative sizes of weights $\{w_m\}$ for $m > N$ compared to $m \leq N$. Here, we will give a method for quantitatively assessing the impact of these surplus noise-only samples on the operating characteristics.

CHARACTERISTIC FUNCTION

The characteristic function of the decision variable is an obvious generalization of (7) to the form

$$f_x(\xi) = \left[\prod_{m=1}^{\infty}\left(1 - i\xi w_m a_m\right)\right]^{-1} , \tag{61}$$

where the signal-to-noise ratio parameter a_m now takes the form

$$a_m = \left\{\begin{matrix} 1 & \text{for noise-alone} \\ 1 + R_m & \text{for signal-plus-noise} \end{matrix}\right\} \quad \text{for } 1 \le m \le M = \infty . \tag{62}$$

The particular case that will be considered at length, here, is that of a finite-duration constant-strength signal, which is accommodated mathematically by setting

$$R_m = \left\{\begin{matrix} R & \text{for} \quad 1 \le m \le N \\ 0 & \text{for} \quad N < m \le M = \infty \end{matrix}\right\} . \tag{63}$$

When signal-to-noise ratio R is equal to zero, that is, signal-absent, the characteristic function in (61) reduces to

$$\tilde{f}_x(\xi) = \left[\prod_{m=1}^{\infty}\left(1 - i\xi w_m\right)\right]^{-1} . \tag{64}$$

Unfortunately, even for the exponential averager,

$$w_m = (1-r)\, r^{m-1} \quad \text{for} \quad 1 \le m \le M = \infty , \tag{65}$$

the noise-only characteristic function in (64) takes a form,

$$f_x(\xi) = \left[\prod_{m=1}^{\infty}\left(1 - i\xi\,(1-r)\,r^{m-1}\right)\right]^{-1}, \qquad (66)$$

which is not expressible in closed form; see [11; (89.18.3)]. (Likewise, the finite product cannot be simplified; see [11; (89.18.2)].) This necessitates termination of the infinite product in (66), being sure to keep the remainder below an acceptable tolerance; this issue is addressed in appendix E.

CUMULANTS

For general characteristic function (61), the cumulants are

$$\frac{1}{(k-1)!}\,\chi_x(k) = \sum_{m=1}^{\infty}(w_m\,a_m)^k \quad \text{for} \quad 1 \le k\ . \qquad (67)$$

For the special case of the exponential averager (65) and the finite-duration signal (63), these cumulants reduce to

$$\frac{1}{(k-1)!}\,\chi_x(k) = \frac{(1-r)^k}{1-r^k}\left[(1+R)^k\left(1-r^{kN}\right) + r^{kN}\right]\ . \qquad (68)$$

At the same time, characteristic function (61) becomes

$$f_x(\xi) = \left[\prod_{m=1}^{N}\left(1 - i\xi\,(1-r)\,r^{m-1}(1+R)\right)\prod_{m=N+1}^{\infty}\left(1 - i\xi\,(1-r)\,r^{m-1}\right)\right]^{-1}\ . \qquad (69)$$

In particular, for noise-alone, then R = 0 and (68) reduces to

$$\frac{1}{(k-1)!}\,\tilde{\chi}_x(k) = \frac{(1-r)^k}{1-r^k} = \frac{(1-r)^{k-1}}{1+r+\ldots+r^{k-1}} \,. \qquad (70)$$

The three lowest-order cases are

$$\tilde{\chi}_x(1) = 1 \,, \quad \tilde{\chi}_x(2) = \frac{1-r}{1+r} \,, \quad \frac{1}{2}\tilde{\chi}_x(3) = \frac{(1-r)^2}{1+r+r^2} \,. \qquad (71)$$

For signal-present, R > 0, the three lowest cumulants are, from (68),

$$\chi_x(1) = 1 + R - R\,r^N \,,$$

$$\chi_x(2) = \frac{1-r}{1+r}\left[(1+R)^2\left(1-r^{2N}\right) + r^{2N}\right] \,,$$

$$\frac{1}{2}\chi_x(3) = \frac{(1-r)^2}{1+r+r^2}\left[(1+R)^3\left(1-r^{3N}\right) + r^{3N}\right] \,. \qquad (72)$$

Here, N is the number of signal components, R is the signal-to-noise ratio per sample, and r is the exponential decay factor for the weight structure (65).

In the evaluation of the signal-present characteristic function (69), the second product will have to be terminated at a finite limit m = L ($\geq$ N). The error due to this truncation is addressed in appendix E.

GRAPHICAL RESULTS

An example of the results in this section for $M = \infty$, $N = 32$, $r = .9$, is displayed in figure 31, as obtained via exact results (66) and (69), along with the truncation procedure of appendix E. Superposed as dashed lines are the results of using the constant plus chi-squared approximation (48), where the parameters are obtained from the cumulants, according to (50). The cumulants themselves are given by (72). The effective number of samples, M_d in (48), takes on the values 10.680, 10.676, 10.673, and 10.672 for the four signal-to-noise ratios of 0, 2, 4, and 6 dB indicated in the figure. This relatively small value of M_d is the reason for the discrepancy in figure 31 between the exact and approximate results.

Figure 32 is drawn for $M = \infty$, $N = 50$, and $r = .96915298$; compare figure 25, for which $M_c = 32$. The values of M_d for the three overlaid curves for signal-to-noise ratios equal to -2, 0, and 2 dB are 33.531, 33.030, and 32.624, respectively. These larger values, for the effective number of samples, lead to better agreement in this figure; in fact, the approximation is in error by only .15 dB along the left edge of the figure.

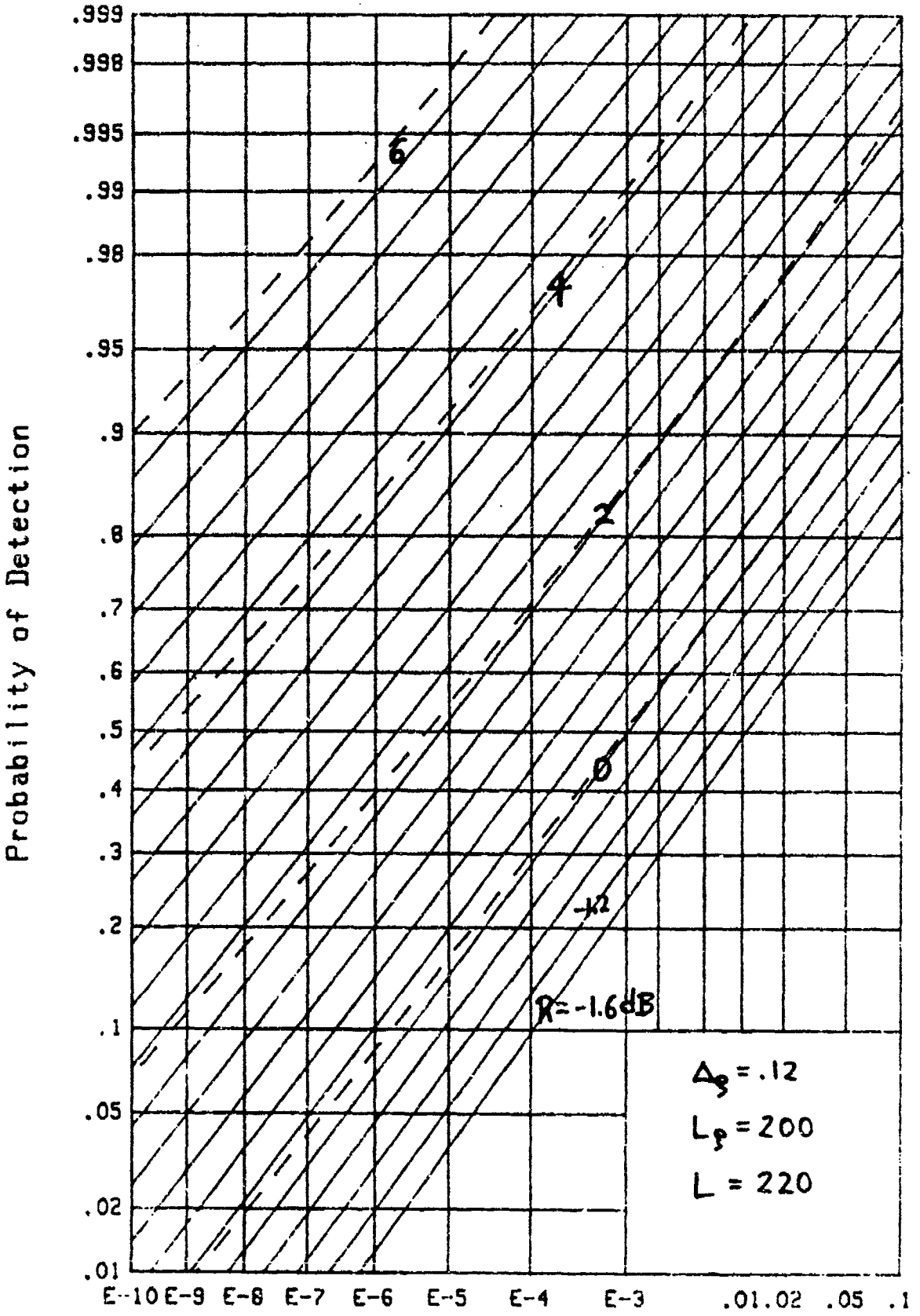

Figure 31. ROC for M=∞, N=32, r=.9

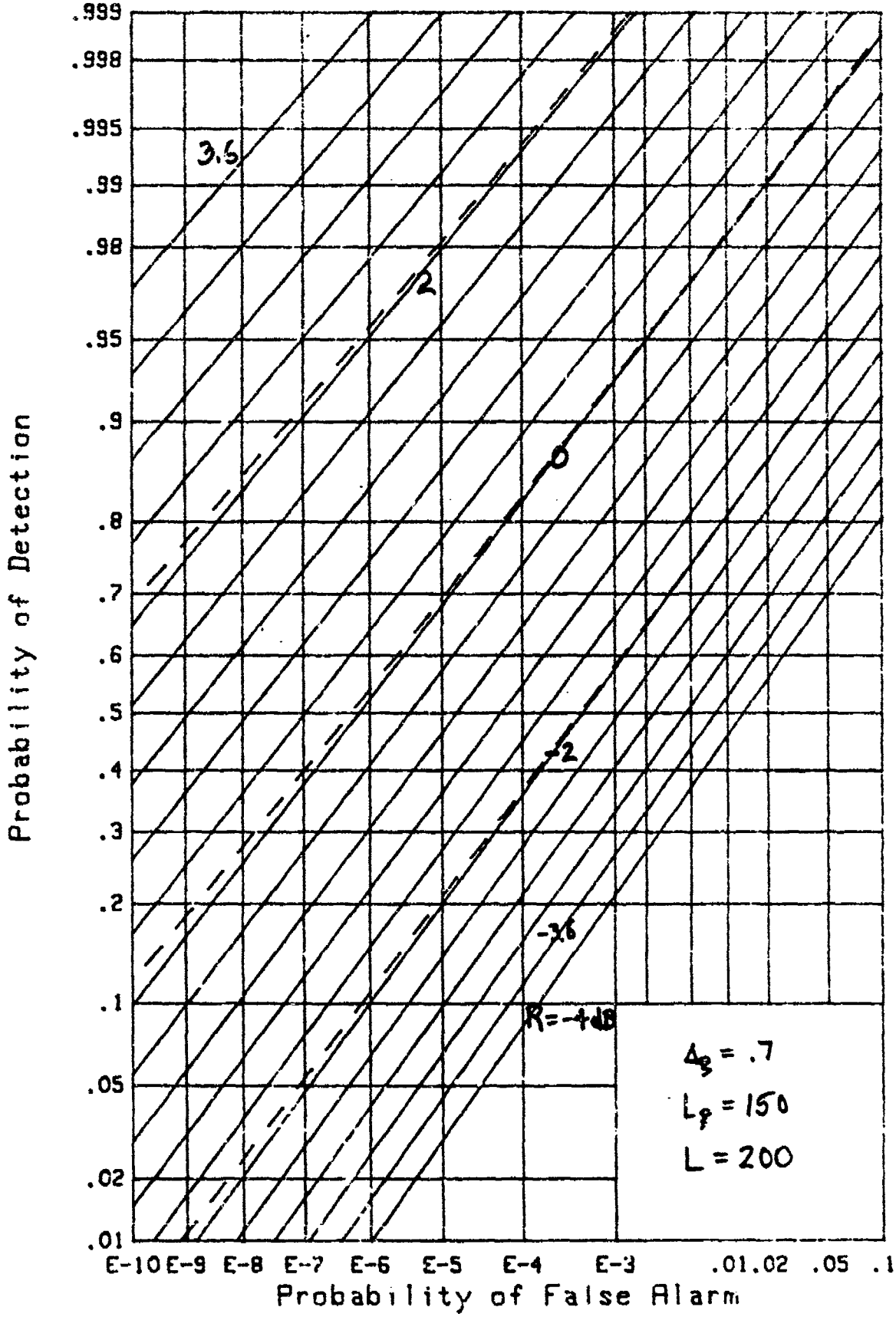

Figure 32. ROC for M=∞, N=50, r=.96915298

BLOCK EXPONENTIAL WEIGHTING

In this section, we again consider a weighted energy detector in steady state, that is, $M = \infty$. However, the averager now operates on blocks of data points which are equally weighted, but which are themselves exponentially weighted. That is, the decision variable x is now given by

$$x = \sum_{m=1}^{\infty} w_m z_m , \tag{73}$$

where the weights $\{w_m\}$ are

$$w_m = \frac{1-r}{B} \begin{Bmatrix} 1 & \text{for} & 1 \le m \le B \\ r & \text{for} & B < m \le 2B \\ r^2 & \text{for} & 2B < m \le 3B \\ \vdots & & \vdots \end{Bmatrix} . \tag{74}$$

Here, B is the block size and the weights have been normalized at $W_1 = 1$. The following diagram illustrates the block exponential weighting structure.

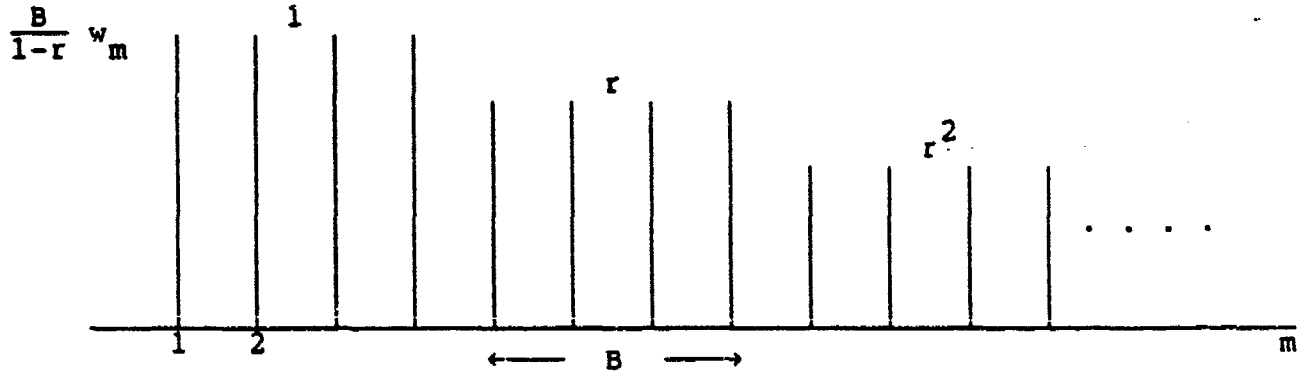

SIGNAL STATISTICS

The signal, if present, occupies the first N samples of sum (73), where

$$J = \frac{N}{B} \tag{75}$$

is presumed integer; that is, J is the number of blocks occupied by signal (when present). The signal-to-noise ratio parameter is

$$a_m = \left\{ \begin{array}{ll} 1 & \text{for noise-only} \\ 1+R & \text{for signal plus noise} \end{array} \right\} \quad \text{for} \quad 1 \leq m \leq N , \tag{76A}$$

and

$$a_m = 1 \quad \text{for} \quad N \leq m < \infty . \tag{76B}$$

CHARACTERISTIC FUNCTION

The characteristic function of x in (73) for signal present is, using the independence of the $\{z_m\}$,

$$f_x(\xi) = \left[\prod_{m=1}^{\infty} \left(1 - i\xi w_m a_m\right) \right]^{-1} =$$

$$= \left[\prod_{j=0}^{J-1} \left(1 - i\xi \frac{1-r}{B} r^j (1 + R)\right) \prod_{j=J}^{\infty} \left(1 - i\xi \frac{1-r}{B} r^j\right) \right]^{-B} . \tag{77}$$

Again, an infinite product is required and the truncation procedure given in appendix E is directly relevant.

CUMULANTS

The cumulants of decision variable x follow readily from (77), upon expansion of $\ln f_x(\xi)$ in a power series in $i\xi$:

$$\frac{1}{(k-1)!}\chi_x(k) = \frac{[(1-r)/B]^{k-1}}{1+r+\cdots+r^{k-1}}\left[(1+R)^k\left(1-r^{kJ}\right) + r^{kJ}\right] \text{ for } k \geq 1. \quad (78)$$

The four lowest-order cumulants will be used in fitting the exact characteristic function (77) by approximations (55) and (58).

GRAPHICAL RESULTS

Results for the operating characteristics for B = 4, J = 32, and r = .95 are presented in figure 33. Thus, from (75), the signal (when present) occurs on N = 128 samples. Superposed as dashed lines is the approximation afforded by third-order fit (33) and (39). The discrepancy is only .1 dB along the left edge of the figure.

Another example of block exponential weighting, for B = 4, J = 16, and r = .9, is displayed in figure 34. The dashed overlay is again the third-order approximation (33), which is optimistic by about .15 dB along the left edge of the figure.

The exact results from figure 34 are repeated in figure 35, but now the overlays are the <u>two</u> fourth-order approximations (55) and (58). The latter two approximations are indistinguishable from each other over the entire range of probabilities displayed. Furthermore, they differ from the exact results only by .05 dB at the left edge of the figure.

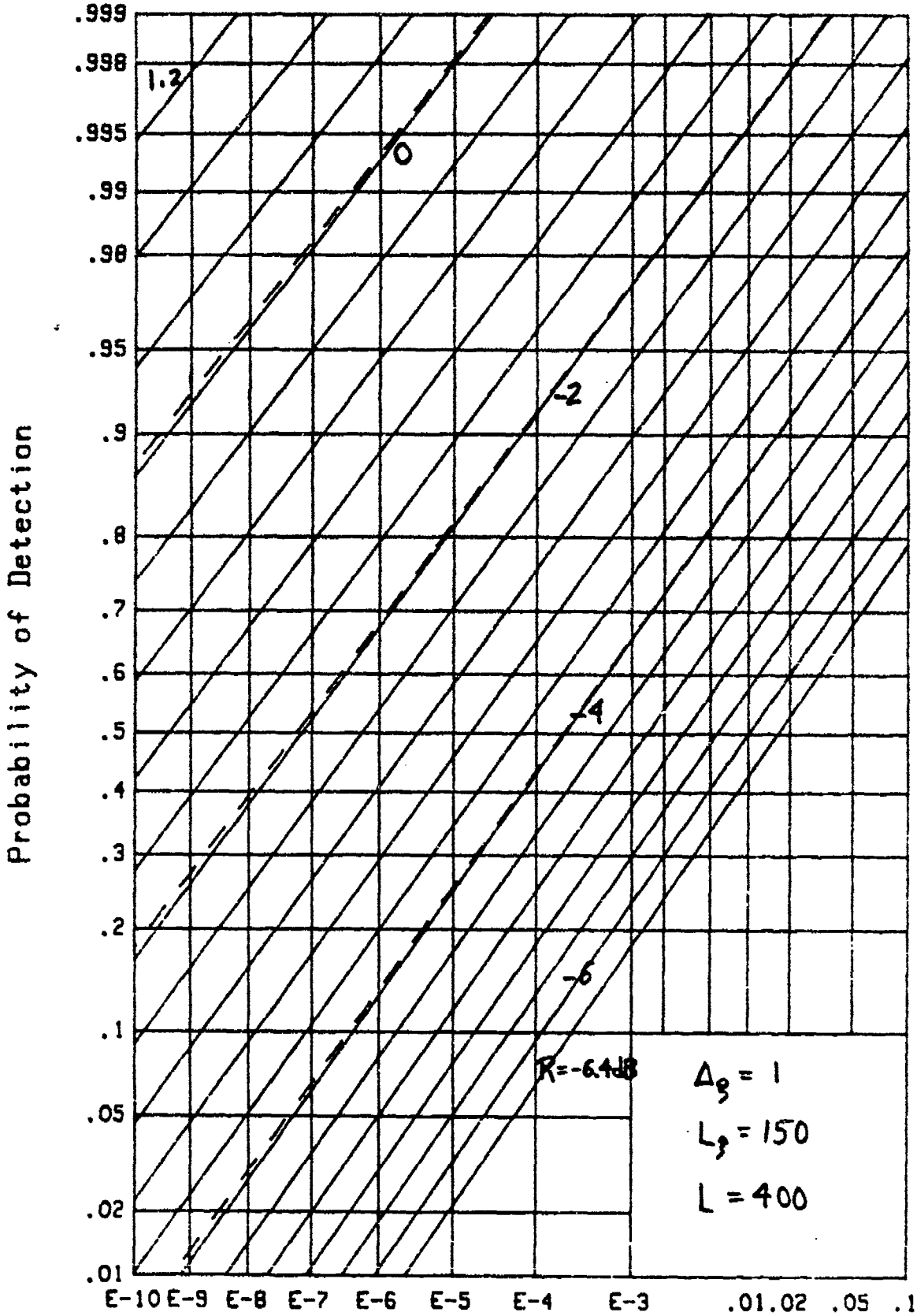

Figure 33. ROC for B=4, J=32, r=.95

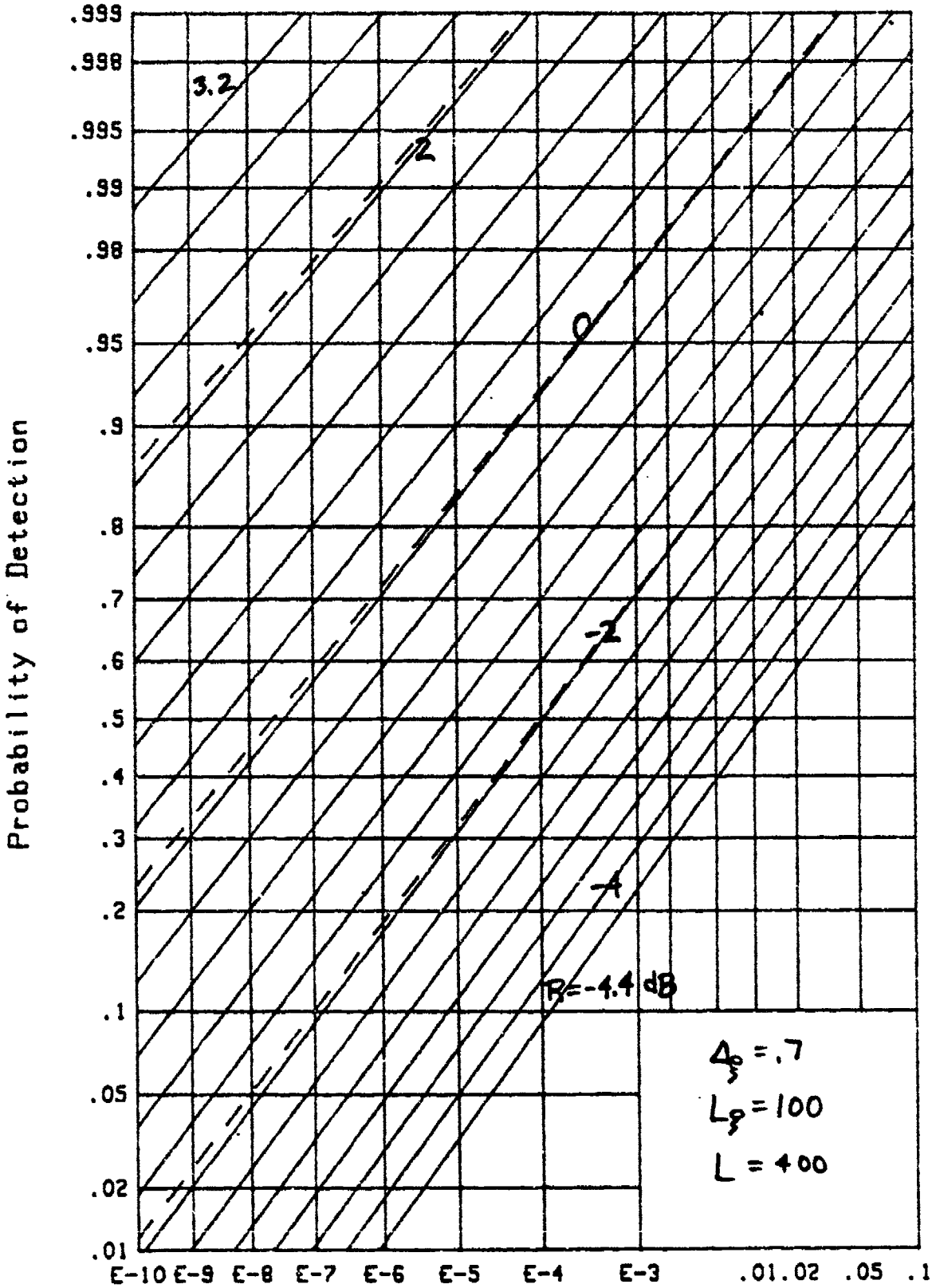

Figure 34. ROC for B=4, J=16, r=.9

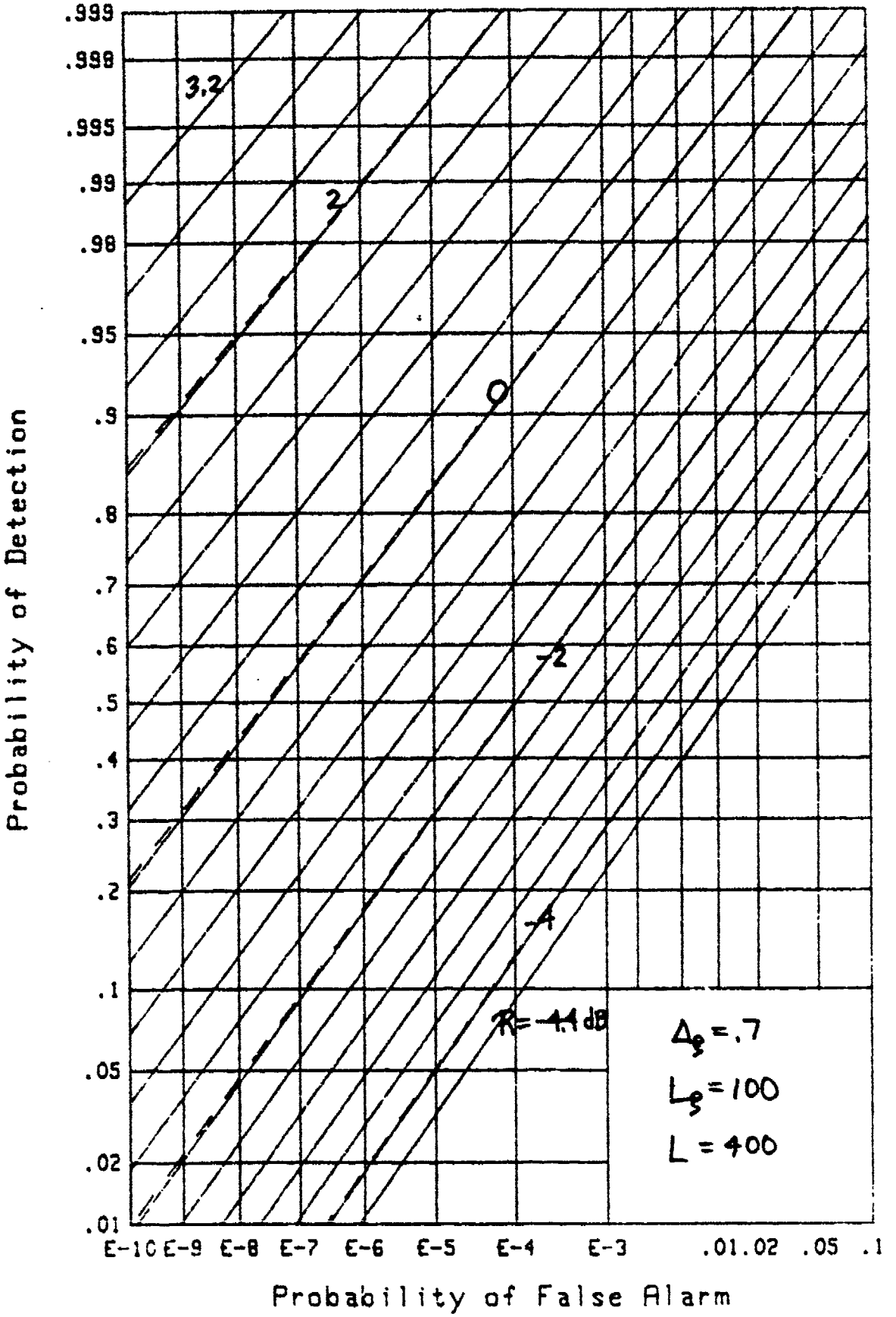

Figure 35. ROC for B=4, J=16, r=.9, fourth-order fits

SUMMARY

The receiver operating characteristics of a variety of weighted energy detectors, for Gaussian signals in noise, have been investigated exactly and compared with five different approximate procedures. The Gaussian and chi-squared approximations have been found to be generally inadequate for very small false alarm probabilities, while the generalized chi-squared (gamma) and both fourth-order fits have yielded very good results over the entire range of detection and false alarm probabilities considered. The only limitation of the latter approaches is the need to have additional cumulants (or moments), since the first two cumulants are not always entirely adequate for accurate performance predictions.

If the exact characteristic function for the decision variable of a system can be determined, either analytically or numerically, then the receiver operating characteristics can be accurately evaluated by the method of [2], as done here. However, there are occasions where it may be desirable or imperative to use an approximate characteristic function, as for example, when only a few low-order moments are known. In this fashion, we can, for example, avoid the determination of eigenvalues or avoid the evaluation of infinite products. Also, the approximate forms will frequently be faster to compute than the exact results. This report indicates the relative accuracies inherent in some of the standard approximations and some of their generalizations, which should be considered for future use.

APPENDIX A - GAUSSIAN APPROXIMATION

The characteristic function of interest was presented in (7):

$$f_x(\xi) = E\{\exp(i\xi x)\} = \prod_{m=1}^{M} f_z(w_m \xi) = \left[\prod_{m=1}^{M} \left(1 - i\xi w_m a\right)\right]^{-1} , \quad (A-1)$$

where $\{w_m\}$, for $1 \le m \le M$, are an arbitrary set of weights. The mean and variance of random variable x were given in (9).

Now, if energy detector output x in (1) were a Gaussian random variable, its probability density function would be

$$p_g(u) = \frac{1}{(2\pi)^{\frac{1}{2}}\sigma_g} \exp\left[-\frac{(u - \mu_g)^2}{2\sigma_g^2}\right] \quad \text{for all } u , \quad (A-2)$$

where, from (9) and (4), we set

$$\mu_g = \left\{ \begin{array}{c} 1 \\ \text{or} \\ 1 + R \end{array} \right\} , \qquad \sigma_g^2 = \left\{ \begin{array}{c} W_2 \\ \text{or} \\ (1 + R)^2 \, W_2 \end{array} \right\} . \quad (A-3)$$

The exceedance distribution function corresponding to (A-2) is

$$Q_g(u) = \int_u^{\infty} dt \; p_g(t) = \Phi\left(\frac{\mu_g - u}{\sigma_g}\right) \quad \text{for all } u , \quad (A-4)$$

where

$$\Phi(t) = \int_{-\infty}^{t} dv \; (2\pi)^{-\frac{1}{2}} \exp(-v^2/2) \quad (A-5)$$

is the normalized Gaussian cumulative distribution function.

At this point, it is convenient to define an effective number of samples, M_e, for an arbitrary set of weights $\{w_m\}$ as in (31)

$$M_e = \frac{\left(\sum_{m=1}^{M} w_m\right)^2}{\sum_{m=1}^{M} w_m^2} = \frac{W_1^2}{W_2} = \frac{1}{W_2} \quad . \tag{A-6}$$

Here, we used (8) and (2).

If threshold T is utilized for a comparison with energy detector output x for a decision on signal presence or absence, then the approximate false alarm probability follows from (A-4):

$$P_F = Q_g(T;\ R=0) = \Phi\left(M_e^{\frac{1}{2}}(1-T)\right) \quad , \tag{A-7}$$

with the help of (A-3) and (A-6). Similarly, the approximate detection probability is

$$P_D = Q_g(T;\ R\neq 0) = \Phi\left(M_e^{\frac{1}{2}}\left(1 - \frac{T}{1+R}\right)\right) \quad . \tag{A-8}$$

Equations (A-7) and (A-8) produce the Gaussian approximation to the operating characteristics of the energy detector (1), described by characteristic function (A-1). They depend only on the single parameter M_e defined in (A-6), in addition to the per-sample signal-to-noise ratio R. That is, M and $\{w_m\}$ are all collapsed into the single parameter, effective number M_e.

An immediate obvious problem with (A-8) is that the limit of detection probability P_D, as $R \to \infty$, is not 1; in fact, it is $\Phi\left(M_e^{\frac{1}{2}}\right) < 1$. This drawback serves as a warning about the adequacy of the Gaussian approximation.

For the approximations in (A-7) and (A-8), we can explicitly solve for P_D in terms of P_F, as follows. Let $\underset{\sim}{\Phi}$ be the inverse function to Φ; see [10; 26.2.23]. Then (A-7) can be solved for threshold T according to

$$T = 1 - M_e^{-\frac{1}{2}} \underset{\sim}{\Phi}(P_F) \ . \tag{A-9}$$

Substitution of this result into (A-8) yields

$$P_D = \Phi\left(\frac{M_e^{\frac{1}{2}} R + \underset{\sim}{\Phi}(P_F)}{1 + R}\right) \ . \tag{A-10}$$

It now follows immediately from (A-10) that, for specified P_F and P_D, the required signal-to-noise ratio R is

$$R = \frac{D - F}{M_e^{\frac{1}{2}} - D} \ , \tag{A-11}$$

where

$$F = \underset{\sim}{\Phi}(P_F) \ , \quad D = \underset{\sim}{\Phi}(P_D) \ . \tag{A-12}$$

The result in (A-11) is a generalization of [1; (C-8) and (11)] to the case of arbitrary weights $\{w_m\}$. It is immediately obvious from the denominator of (A-11) that the desired P_D must be smaller than $\Phi\left(M_e^{\frac{1}{2}}\right)$.

APPENDIX B - POSITIVITY OF PARAMETER b_c

Here, we will show that the parameter b_c in (35) is never negative, regardless of the weight structure $\{w_m\}$, provided that $w_m \geq 0$. The Cauchy-Schwartz inequality states that

$$\left(\sum_{m=1}^{M} a_m b_m\right)^2 \leq \sum_{m=1}^{M} a_m^2 \sum_{m=1}^{M} b_m^2 \qquad \text{(B-1)}$$

for any real quantities $\{a_m\}$ and $\{b_m\}$. If we let $a_m = w_m^{3/2}$ and $b_m = w_m^{1/2}$, then (B-1) yields

$$\left(\sum_{m=1}^{M} w_m^2\right)^2 \leq \sum_{m=1}^{M} w_m^3 \sum_{m=1}^{M} w_m \,, \qquad \text{(B-2)}$$

that is, $W_2^2 \leq W_3 W_1$, where

$$W_k = \sum_{m=1}^{M} w_m^k \,. \qquad \text{(B-3)}$$

Therefore

$$b_c = W_1 - \frac{W_2^2}{W_3} \geq 0 \,. \qquad \text{(B-4)}$$

In addition, there follows

$$M_c w_c = \frac{W_2^2}{W_3} \leq W_1 \,. \qquad \text{(B-5)}$$

APPENDIX C - TRACE RELATIONS FOR EIGENVALUES

Suppose MxM matrix $P = [\rho_{mn}]$ has eigenvalues $\{\lambda_m\}$, $1 \leq m \leq M$. Let Λ be the diagonal matrix of eigenvalues $\{\lambda_m\}$ and let Q be the normalized modal matrix of eigenvectors of P; see [12; section 1.13]. Then we can express matrix P in the form

$$P = Q \Lambda Q^T , \tag{C-1}$$

from which there follows the k-th power

$$P^k = Q \Lambda^k Q^T . \tag{C-2}$$

We now use the trace relation

$$tr(A\ B\ C) = tr(B\ C\ A) , \tag{C-3}$$

to evaluate the trace of P^k:

$$tr(P^k) = tr(Q\ \Lambda^k\ Q^T) = tr(\Lambda^k\ Q^T\ Q) = tr(\Lambda^k) = \sum_{m=1}^{M} \lambda_m^k . \tag{C-4}$$

That is, the sum of the k-th powers of eigenvalues $\{\lambda_m\}$ can be obtained from the trace of matrix P^k, without ever having to evaluate the eigenvalues at all. In particular,

$$\sum_{m=1}^{M} \lambda_m = tr(P) = \sum_{m=1}^{M} \rho_{mm} , \tag{C-5}$$

$$\sum_{m=1}^{M} \lambda_m^2 = tr(P^2) = \sum_{m,n=1}^{M} \rho_{mn}\ \rho_{nm} , \tag{C-6}$$

$$\sum_{m=1}^{M} \lambda_m^3 = tr(P^3) = \sum_{m,n,k=1}^{M} \rho_{mn}\ \rho_{nk}\ \rho_{km} \cdot \qquad (C\text{-}7)$$

In order to compute the sums of the three lowest powers of the eigenvalues of matrix P, we simply have to compute the three sums on the elements of matrix P, as indicated in (C-5) through (C-7). In fact, there is no need to compute matrices P^2 or P^3 either. Thus, a seemingly difficult numerical chore is replaced by straightforward simple summations of products of matrix elements, yielding a very significant savings in complexity and time.

APPENDIX D - INVERSION OF EQUATION (60)

For notational efficiency, we suppress all the g subscripts in (60), let $y_k = X(k)/(k-1)!$, and set $p = M\,w$. The nonlinear equations then take the form

$$y_1 = b + p\ , \quad y_2 = 2\,b\,c + p\,w\ ,$$
$$y_3 = 3\,b\,c^2 + p\,w^2\ , \quad y_4 = 4\,b\,c^3 + p\,w^3\ . \qquad \text{(D-1)}$$

We solve the first two equations for p and b, getting

$$p = \frac{y_2 - 2\,y_1\,c}{w - 2\,c}\ , \quad b = \frac{y_1\,w - y_2}{w - 2\,c}\ . \qquad \text{(D-2)}$$

These quantities are now substituted in the third and fourth equations in (D-1), resulting in the highly nonlinear pair of coupled equations for c and w:

$$c^2\,3\,(y_1\,w - y_2) + c\,2\,(y_3 - y_1\,w^2) + w\,(y_2\,w - y_3) = 0\ , \qquad \text{(D-3)}$$
$$c^3\,4\,(y_1\,w - y_2) + c\,2\,(y_4 - y_1\,w^3) + w\,(y_2\,w^2 - y_4) = 0\ . \qquad \text{(D-4)}$$

The procedure we have adopted for solving these latter two equations is to start with an initial guess for w as in (57), namely

$$w = \frac{X(4)/6}{X(3)/2} = \frac{y_4}{y_3}\ ; \qquad \text{(D-5)}$$

then solve quadratic (D-3) for c; substitute this result into (D-4) and compute the left-hand side; now vary w until the left-hand side equals zero. Repeat these operations until c and w stabilize. Equation (D-2) can now be used to get final values of p and b. This is the numerical procedure used in the main text.

APPENDIX E - TERMINATION OF INFINITE PRODUCT

If we terminate the infinite product for the characteristic functions in (66) or (69) at limit value $m = L\ (\geq N)$, then the neglected remainder product in the denominator is

$$\text{Rem} = \prod_{m=L+1}^{\infty}\left(1 - i\xi\,(1-r)\,r^{m-1}\right) = 1 - i\xi r^{L} - \xi^{2}\,\frac{r^{2L+1}}{1+r} + O\left(r^{3L}\right). \quad \text{(E-1)}$$

This relation enables a choice of L to control the neglected remainder. For example, $\xi = 200$, $L = 220$, $r = .9$ leads to Rem = 1 - i1.7E-8 - 1.4E-16. Thus, the ξ^2 term and above can be safely ignored. One final product in the denominator of (66), by the factor $1 - i\xi r^{L}$, will account for Rem and suffice for complete accuracy, up to computer round-off error in the characteristic function evaluation. For larger values of r, it is necessary to increase the limit L; for example, $\xi = 150$, $L = 700$, $r = .96915298$ yields Rem = 1 - i4.5E-8 - 1E-15.

If we terminate the infinite product for the characteristic function in (77) at limit value $j = L\ (\geq J-1)$, the neglected remainder product in the denominator is

$$\text{Rem} = \left[\prod_{j=L+1}^{\infty}\left(1 - i\xi\,\frac{1-r}{B}\,r^{j}\right)\right]^{B} \sim \left(1 - \frac{i\xi}{B}\,r^{L+1}\right)^{B} \sim 1 - i\xi\,r^{L+1}. \quad \text{(E-2)}$$

This is substantially the same as (E-1), where terms of the order of r^{2L} have been neglected.

REFERENCES

[1] A. H. Nuttall and A. F. Magaraci, **Signal-to-Noise Ratios Required for Short-Term Narrowband Detection of Gaussian Processes**, NUSC Technical Report 4417, Naval Underwater Systems Center, New London, CT, 20 October 1972.

[2] A. H. Nuttall, **Accurate Efficient Evaluation of Cumulative or Exceedance Probability Distributions Directly From Characteristic Functions**, NUSC Technical Report 7023, Naval Underwater Systems Center, New London, CT, 1 October 1983.

[3] A. H. Nuttall, **Exact Performance of General Second-Order Processors for Gaussian Inputs**, NUSC Technical Report 7035, Naval Underwater Systems Center, New London, CT, 15 October 1983.

[4] A. H. Nuttall and B. Dedreux, **Exact Operating Characteristics for Linear Sum of Envelopes of Narrowband Gaussian Process and Sinewave**, NUSC Technical Report 7117, Naval Underwater Systems Center, New London, CT, 11 January 1984.

[5] A. H. Nuttall, **Operating Characteristics of Cross-Correlator With or Without Sample Mean Removal**, NUSC Technical Report 7045, Naval Underwater Systems Center, New London, CT, 14 August 1984.

[6] A. H. Nuttall, **Probability Distribution of Spectral Estimates Obtained via Overlapped FFT Processing of Windowed Data**, NUSC Technical Report 5529, Naval Underwater Systems Center, New London, CT, 3 December 1976.

[7] A. H. Nuttall, **Operating Characteristics for Detection of a Fading Signal with K Dependent Fades and D-fold Diversity in M Alternative Locations**, NUSC Technical Report 5739, Naval Underwater Systems Center, New London, CT, 25 October 1977.

[8] I. Kanter, "Exact Detection Probability for Partially Correlated Rayleigh Targets", **IEEE Transactions on Aerospace and Electronics Systems**, volume AES-22, number 2, pages 184 - 195, March 1986.

[9] A. H. Nuttall and E. S. Eby, **Signal-to-Noise Ratio Requirements for Detection of Multiple Pulses Subject to Partially Correlated Fading With Chi-Squared Statistics of Various Degrees of Freedom**, NUSC Technical Report 7707, Naval Underwater Systems Center, New London, CT, 2 June 1986.

[10] **Handbook of Mathematical Functions**, U. S. Department of Commerce, National Bureau of Standards, Applied Mathematics Series Number 55, U. S. Government Printing Office, Washington, DC, June 1964.

[11] E. R. Hansen, **A Table of Series and Products**, Prentice-Hall, Inc., Englewood Cliffs, NJ, 1975.

[12] F. B. Hildebrand, **Methods of Applied Mathematics**, Prentice-Hall, Inc., New York, NY, 1954.